

Increasing opal productivity in the late Eocene Southern Ocean: Evidence for increased carbon export preceding the Eocene-Oligocene glaciation

Volkan Özen^{1,2}, [Johan Renaudie](#)², David B. Lazarus², [Johan Renaudie](#)², Gabrielle Rodrigues de Faria^{1,2}

⁵ Freie Universität Berlin, Institute for Geological Sciences, Malteserstraße 74–100, 12249 Berlin, Germany

² Museum für Naturkunde, Leibniz Institute for Evolution and Biodiversity Science, Invalidenstraße 43, 10115 Berlin, Germany

Correspondence to: Volkan Özen (volkan.oezen@fu-berlin.de)

10

Abstract. The Eocene/Oligocene Transition represents a period of profound changes in diatom productivity and evolutionary history within the Cenozoic era. Unraveling how these changes correlate with climatic shifts during this transition is crucial for understanding the potential role of diatoms in the cooling trends observed at the Eocene/Oligocene boundary (~33.9 Ma). Current research predominantly relies on bulk opal accumulation measurements to assess productivity dynamics, which fails to distinguish the contribution of different biosiliceous (e.g., diatom versus radiolarian) plankton to total biogenic silica productivity. Furthermore, despite the fundamental role of community composition and diversity in diatom productivity and carbon sequestration, these factors are often not incorporated in existing studies focusing on the late Paleogene diatom productivity. The main objective of our work is to explore the potential roles of diatom communities in the late Eocene climatic changes by focusing on diatom- and radiolarian-specific productivity across multiple Southern Ocean sites, rather than bulk opal measurements, and by incorporating total diatom abundance into the analysis of diatom diversity evolution throughout the Eocene/Oligocene transition. By quantifying diatom and radiolarian abundances across four Southern Ocean sites in the Atlantic and Indian Ocean sectors, and analyzing diatom productivity through recent reconstructions of diatom diversity from approximately 40–30 Ma interval, our findings reveal a significant increase in diatom abundance coupled with notable shifts in community diversity. These changes suggest a potential ecological shift, likely associated with the development of stronger circum-Antarctic currents in the late Eocene. Such shifts could have influenced the efficiency of the biological carbon pump by enhancing organic carbon export to the deep ocean and thus potentially contributing to reduced atmospheric CO₂ levels. While our findings indicate that the expansion of diatoms may have been a part of the mechanisms underlying the late Eocene cooling, they also highlight the importance of integrating diatom diversity and community evolution into diatom productivity research. Furthermore, our results offer valuable insights into the complex relationship between diatom abundance and diversity in the geological record, reflecting the intricate interplay of environmental and climatic factors.

1 Introduction

35 The Eocene/Oligocene boundary (E/O, ~33.9 Ma) marks the end of the Cenozoic Hothouse with high-latitude surface ocean cooling and an abrupt 1.5 per mil increase in global benthic $\delta^{18}\text{O}$ values (Shackleton and Kennett, 1975; Zachos et al., 1996, 2001; Coxall et al., 2005; Zachos and Kump, 2005; Coxall and Pearson, 2007; Liu et al., 2009; Westerhold et al., 2020; Hutchinson et al., 2021). It corresponds to the largest cooling shift of the late Paleogene gradual cooling trend and the abrupt emplacement/expansion of the Antarctic ice sheet (Lear et al., 2008). Despite the ~~extensive research~~~~large volume of research describing the environmental mosaic of the E/O transition~~, the underlying mechanisms are under dispute. The discussions on the possible ~~mechanism~~~~causes of the abrupt climatic state shift~~ have revolved around ~~three~~~~two~~ main domains (1) gradual thermal isolation of Antarctica with the development of the Antarctic Circumpolar Current (ACC) initiated by the deepening of the Southern Ocean ([here and after](#) SO) gateways (Kennett, 1977; Barker, 2001), ~~and~~ (2) the threshold response of the Earth climate to the atmospheric CO₂ decrease in the late Paleogene (DeConto and Pollard, 2003; 45 [Ladant et al., 2014](#)), ~~and~~ (3) [the evolution of the west Antarctic rift system, which might have significantly modulated ice-sheet volume and climate feedbacks \(Wilson and Luyendyk, 2009; Wilson et al., 2013\)](#).

50 Proposed [These](#) mechanisms underlying the E/O transition are ~~not mutually exclusive~~~~possibly interlinked~~; and both oceanographic changes, ~~and~~ CO₂ [drawdown](#), and [tectonic reorganization of Antarctic topography are supported and extensively discussed by proxy records and model results as the overriding mechanism have support \(e.g.,](#) Scher and Martin, 2006; Ladant et al., 2014; Elsworth et al., 2017; [Paxman et al., 2019](#); Toumoulin et al., 2020; Hutchinson et al., 2021; Lauretano et al., 2021; [Klages et al., 2024](#))

55 [Within this broader framework, several studies have suggested that increased SO productivity may have contributed to CO₂ decline by linking changes in circulation to export productivity and carbon sequestration \(e.g.,](#) Diester-Haass and Zahn, 1996; [Salamy and Zachos, 1999](#); [Schumacher and Lazarus, 2004](#); [Egan et al., 2013](#); [Rodrigues de Faria et al., 2024](#))

60 [Although the timing and characteristics of this productivity shift remain debated \(Renaudie, 2016; Wade et al., 2020; Brylka et al., 2024,; Rodrigues De Faria et al., 2024\), it was likely a piece of the broader mechanistic mosaic underlying the E/O transition and Antarctic glaciation.](#)

[Diatoms and radiolarians, as major siliceous plankton groups, are pivotal to these discussions, both as contributors to export production and as proxies for changing nutrient supply and ocean circulation. Their fossil records suggest significant reorganization across the late Eocene to early Oligocene interval \(see Section 1.2\).](#)

65 [The existing literature on the onset of the ACC is extensive and focuses particularly on the deepening of Southern Ocean gateways \(e.g., Kennett, 1977; Stieckley et al., 2004; Sijp et al., 2011; Evangelinos et al., 2022\).](#) Sufficiently deep gateways would develop a circulation system akin to the ACC, and pave the way for a stronger latitudinal thermal gradient and thermal isolation of the Antarctic continent (Sauermilch et al. 2021).

A significant challenge for the proto-ACC isolation hypothesis lies in the poorly constrained timing of the SO gateway openings. Although the Tasman gateway is thought to have been substantially open by ca 35 Ma (Stickley et al., 2004), the timing of Drake Passage opening remains highly debated, with estimates ranging from mid Eocene to basal Neogene (e.g., Scher and Martin, 2006; Livermore et al., 2007; Barker et al., 2007; Scher et al., 2015; Hodel et al., 2021).

70

On the other hand, the main difficulty with the CO₂ line of reasoning, as the overriding mechanism, is that, while the CO₂ reconstructions are accepted at face value, the possible mechanism(s) underlying the late Eocene drawdown in CO₂ is not well constrained. It is indeed conceivable that these two domains of possible mechanisms were probably linked: a gradual increase in proto-ACC strength would increase ocean mixing rates and, thus, mixed-layer thickness. Consequently, increasing mixing rates and related upwelling systems would promote SO plankton productivity and thus organic carbon sequestration (via biological carbon pump) into the deep ocean and sediments, and thus to the atmospheric CO₂ drawdown (e.g., Scher and Martin, 2006; Egan et al., 2013; Rodrigues de Faria et al., 2024).

75

80

The critical point is that a modest decrease in CO₂ may have been sufficient to trigger the threshold response observed at the E/O. Previous studies indicate that CO₂ levels in the late Eocene declined significantly, reaching as low as ~800 ppm (Anagnostou et al., 2016), which approaches the model-estimated threshold of ~750 ppm required for E/O cooling and the onset of (primarily East) Antarctic glaciation (DeConto et al., 2008). Therefore, the role of increasing, particularly diatoms, SO productivity (Salamy and Zachos, 1999; Schumacher and Lazarus, 2004; Egan et al., 2013; Rodrigues de Faria et al., 2024) stands out as a critical mechanism that might have contributed to the final increment in CO₂ drawdown, consequently to E/O cooling, although its timing and characteristics remain a matter of contention.

85

1.1 Opal as a paleoproductivity proxy

90

Biosiliceous Biogenic silica deposition in modern open-ocean settings oceans reflects closely correlates with the surface ocean productivity dynamics of the overlying water column, a pattern observed consistently across diverse regions from the equatorial to high-latitude Pacific and Atlantic Oceans (Baldauf and Barron, 1990; Barron et al., 2015). Biogenic silica has significantly higher preservation potential than organic carbon (Tréguer et al., 1995; Ragueneau et al., 2000 and references therein), signifying the potential of biogenic silica deposition and its secular trends in tracking the changing paleoproductivity trends throughout the Cenozoic. However, using opal as a paleoproductivity this proxy is complicated by spatial and temporal variations variability in silica dissolution and preservation, as well as the decoupling of the silica-carbon relationship from surface waters to sediments (Ragueneau et al., 2000). The factors influencing silica dissolution and preservation are not fully constrained and are expected to vary significantly under different oceanographic and climatic conditions throughout the Cenozoic (Ragueneau et al., 2000; Westacott et al., 2021). Although the links between the tempo and mode of opal deposition, and productivity dynamics are complex, it has been shown that the secular trend of opal

deposition is closely related with the global oceanographic and climatic changes (Cortese et al., 2004). Additionally, the 100 evolutionary history of biosiliceous plankton underlying opal deposition during the Cenozoic is a critical but often overlooked aspect in paleoproductivity interpretations based on opal accumulation. Most available data are based on bulk opal measurements, which can obscure the contributions of different biosiliceous plankton groups, such as radiolarians (another extremely important siliceous plankton) and marine diatoms. Assessing the relative contributions of different biosiliceous plankton groups to opal sedimentation is essential for accurate paleoproductivity reconstructions (Ragueneau et 105 al., 2000, 2006).

1.2 Prior opal records and the role of diatom diversity in Southern Ocean productivity Prior opal records from the Southern Ocean Paleogene and their limitations

~~E~~Considerable evidence ~~from the~~ has been accumulated showing that SO suggests that productivity in the region increased across the ~~the~~ during the late Eocene, with the first notable shifts occurring around 38–37 Ma (Diester-Haass and 110 Zahn, 1996; Schumacher and Lazarus, 2004; Villa et al., 2014; Rodrigues de Faria et al., 2024). The rise in opal deposition during the late Eocene and at the E/O (Salamy and Zachos, 1999; Diekmann et al., 2004; Anderson and Delaney, 2005; Brylka et al., 2024), has been linked to the growing dominance of diatoms in open ocean settings. Given the 115 central role of modern diatoms in carbon export through the biological carbon pump (e.g., Tréguer et al., 2018), these observations have drawn attention to a possible link between increased diatom productivity and atmospheric CO₂ decline at the E/O (Salamy and Zachos, 1999; Scher and Martin, 2006; Rabosky and Sorhannus, 2009; Egan et al., 2013; Renaudie, 2016). However, utilizing the opal deposition history to elucidate the diatom productivity across the 120 end-Eocene remains challenging because the data so far is based on bulk opal measurements which do not allow to assess the relative contribution of diatoms and other siliceous plankton, especially radiolarians. Although diatoms dominate opal sedimentation in modern oceans, radiolarians were more common in the early Paleogene, and the shift to diatom dominance occurred during a poorly constrained interval in the mid to late Paleogene (Renaudie, 2016). Data suggest that the first pronounced changes in the SO productivity started between 38 and 37 Ma (Diester-Haass and 125 Zahn, 1996; Diekmann et al., 2004; Anderson and Delaney, 2005; Rodrigues de Faria et al., 2024). The concurrent increase in opal productivity, when combined with the key role of modern diatoms in carbon sequestration via biological carbon pump (Tréguer et al., 2018), motivated the hypothesis that increased diatom productivity, and thus the opal sedimentation, might have contributed to the CO₂ drawdown across the E/O transition (e.g., Egan et al., 2013). Indeed, the data so far show 130 that the first pronounced increase in Cenozoic diatom abundance occurred at the E/O boundary (Renaudie, 2016). Further, based on diatom Si geochemistry, it has been proposed that SO diatom productivity increased during the late Eocene (Egan et al., 2013). However, a recent diversity survey has suggested that observed changes in silicic acid measurements may reflect shifts in community composition rather than, or in addition to, increased productivity (Özen et al., subm.).

In the Indian Ocean sector, Salamy and Zachos (1999) (ODP Site 744A) showed that opal deposition profoundly increased right before the E/O boundary. A recent data from the same region (ODP Site 748B) show strong agreement in opal accumulation trends, reinforcing the robustness of these records (Brylka et al., 2024). However, utilizing the opal deposition history to elucidate the diatom productivity across the end Eocene is problematic because the data so far is based on bulk opal measurements which do not allow to assess the relative contribution of diatoms and other siliceous plankton, especially radiolarians. Although in modern oceans opal sedimentation is dominated by diatoms, data suggest radiolarian dominated communities in the early Paleogene, and the shift to diatom dominance occurring in a poorly constrained interval in the mid to late Paleogene (Renaudie, 2016).

1.3 Links between biodiversity, abundance and productivity

It has been suggested that community diversity in diatoms is important for the overall abundance and productivity, and this for the efficiency of the biological carbon pump (Tréguer et al., 2018). This in accord with the frequently, if not universally, seen pattern of a positive, or 'hump-shaped', correlation between diversity and productivity in many groups of organisms, particularly groups of plants on global scales (Mittelbach et al., 2001). Indeed, in paleontological studies, diatom diversity has often been used as a proxy for abundance (e.g., Lazarus et al., 2014). In a work based on benthic diatom communities, it has been shown that there is a positive link between diverse communities and biomass production (Virta et al., 2019). Moreover, it has been shown that diversity might promote stability in community dynamics (Hatton et al., 2024), this in turn, community stability would presumably lead to a sustained periods high level overall productivity. Although a link between diverse communities and abundance/productivity is a fundamental concept in plankton studies, the details of this link are yet poorly understood. For instance, molecular estimates on global diatom distribution and abundance in different oceanic settings suggest that diatom diversity in eutrophic areas are comparable to the numbers seen in oligotrophic settings (Malviya et al., 2016). The presumed link between diatom diversity and abundance in paleo communities thus needs to be critically investigated. In our study, we combine our diatom abundance data with a recent diversity survey of the late Eocene and early Oligocene SO diatoms (Özen et al., subm.), giving us a ground to provide new insights into diatom-climate interactions at the end Eocene.

The role of diatom diversity in driving productivity is also poorly constrained and often overlooked in paleoproductivity studies. Most reconstructions addressing late Paleogene opal deposition do not distinguish among siliceous groups and remain agnostic to the species diversity underlying the opal signal (Salamy and Zachos, 1999; Diekmann et al., 2004; Anderson and Delaney, 2005; Plancq et al., 2014). Yet in modern ecosystems, diverse plankton communities are associated with higher biomass production, carbon export, and greater ecological stability (Tréguer et al., 2018; Virta et al., 2019; Hatton et al., 2024). A positive, often unimodal, relationship between diversity and productivity has been documented across many taxa, particularly groups of plants on global scales (Mittelbach et al., 2001). However, in paleoceanography, the link between diatom diversity and abundance/productivity is not well understood. Diatom diversity has at times been used as a proxy for abundance (Lazarus et al., 2014), tough molecular data complicate this assumption by showing comparable diversity values in both eutrophic and oligotrophic settings

165 | (Malviya et al., 2016). These findings point to the need to re-evaluate the diversity-productivity relationship in fossil
plankton communities using direct, paired observations.

170 | Constraining the In this study, we aim to improve constraints on SO diatom productivity across the late Eocene–early
Oligocene interval by distinguishing the relative contributions of diatoms and radiolarians to total biogenic silica
deposition. We present newly generated mass accumulation rate (MAR) data for both groups, based on the same
sediment samples used in recent biological barium (bio-Ba) reconstructions (Rodrigues de Faria et al., 2024). By
comparing these group-specific accumulation records with bulk opal and bio-Ba productivity estimates, we provide
an independent assessment of siliceous plankton dynamics across the transition. Finally, we explore the relationship
between diatom abundance and diversity to discuss the long-presumed link between diatom diversity and abundance.
175 | is one of the central research themes addressing the mechanisms underlying the E/O transition. As diatoms, as primary
producers, presumably play a greater role in carbon capture than an equivalent cellular mass of other siliceous
plankton, discriminating the relative contribution of different siliceous plankton to the total opal sedimentation is
therefore an important step to constrain diatom productivity and its possible role at the E/O transition. Here, we
180 | present diatom and radiolarian productivity patterns across the E/O transition based on newly generated
accumulation rates. We combine our results with previously published opal bulk accumulation rates to assess the
relative contribution of these groups to overall siliceous productivity. Recently generated productivity values based
on biological barium (bio-Ba) (Rodrigues de Faria et al., 2024), from the same samples we used to generate our data,
give us an independent control in interpreting our productivity data. Moreover, we compare the diatom abundances
across the E/O transition to discuss the long-presumed link between diatom diversity and abundance.

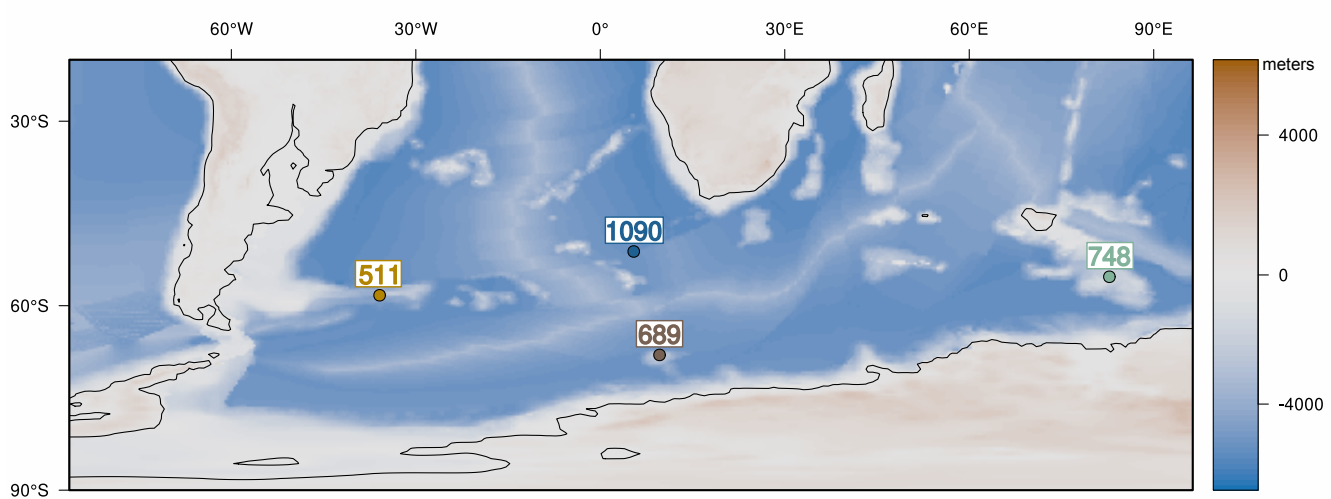
185 | **2 Methods**

186 | **2.1 Material**

187 | We analyzed diatom and radiolarian abundance data from samples collected from the following SO sites: Deep Sea Drilling
Project (DSDP) Site 511 (Falkland Plateau, 51°00.28'S; 46°58.30'W) (sampled interval ~27–180 meter below sea floor
(mbsf)), Ocean Drilling Project (ODP) Site 1090B (Agulhas Ridge, 42°54.8'S 8°53.9'E) (~188–335 mbsf), ODP Site 748B
190 | (Kerguelen Plateau, 58°26.45'S; 78°58.89'E) (~96–171 mbsf), and ODP Site 689D (Maud Rise, 64°31'S 3°6'E) (~104–132
mbsf) (Fig. 1). Our study examines 53 samples spanning the temporal interval from the late Eocene to the early Oligocene,
approximately between 39 and 30 Ma, with site-specific coverage varying due to differences in sedimentation history at each
site.

195 | DSDP Site 511 (Falkland Plateau) and ODP Site 1090 (Agulhas Ridge) contain hiatuses in the earliest Oligocene, limiting
the temporal coverage of these sites. At DSDP 511, our samples temporal coverage is ~37.5–32.5 Ma. Similarly, at Site

1090, the sampled interval spans ~38—33 Ma, with a hiatus restricting samples from extending well into the Oligocene. In
200 contrast, at ODP Site 689 (Maud Rise) and ODP Site 748 (Kerguelen Plateau), sedimentation is relatively continuous,
providing a more complete record of the EOT (~36.5—30 Ma at Site 689; ~40—29 Ma at Site 748). All analyzed samples
and corresponding measurements, including diatom and radiolarian abundance data, are detailed in the Supplementary
Materials.



In the southern high latitudes, DSDP Site 511 and ODP Site 1090 are notable for being a major locus of biogenic silica deposition across the Eocene/Oligocene transition (e.g., Diekmann et al., 2004; Anderson and Delaney, 2005; Renaudie, 2016; Wade et al., 2020). While ODP Site 689D and 748B, in general, do not exhibit the same level of opal productivity, significant productivity changes have been documented at these sites across the E/O transition (e.g., Salamy and Zachos, 1999; Brylka et al., 2024). These findings signify that these sites provide invaluable insights into the SO productivity in the areas proximal to the Antarctic continent. They provide essential insights into how opal productivity varies under different regional settings, offering a broader perspective on productivity changes across the SO.

215 A comprehensive overview of the updated age models used in this study for each Hole/Site is available in Rodrigues de Faria et al. (2024); see also Supplementary Text 1. The models can also be accessed via the Neptune Database (Renaudie et al., 2020, 2023). Paleobathymetry at each site at the E/O boundary was computed using those age models and each hole lithological descriptions from their corresponding Initial Reports (Shipboard Scientific Party 1983, 1988, 1989, 1999) using PyBacktrack (Müller et al. 2018). The files used as input for PyBackTrack can be found in the 220 SOM, as well as its output.

2.1.1 Sample Preparation

Microscope slides for counting diatom and radiolarian abundances were prepared following a modified version of the methods described by Moore (1973) and Lazarus (1994) and sieved using a 10 μm sieve. About 0.5–1 gram sediment was treated with hydrogen peroxide (H_2O_2) and pentasodium triphosphate ($\text{Na}_5\text{P}_3\text{O}_{10}$) over heat, followed by treatment with hydrochloric acid (HCl). The resulting solution was then sieved through a 10 μm sieve. A controlled amount of the residues was then gently settled over three coverslips at the bottom of a beaker. This approach ensures the material settles randomly across the coverslips, minimizing potential biases that might arise during the enumeration phase (for details, see Lazarus, 1994).

2.2 Diatom and radiolarian absolute abundance and accumulation rates

Absolute abundances (ab) for diatoms and radiolarians were calculated by counting specimens on a known area of slides, following the equation below:

$$\text{ab} = N \times (\text{Ab}/\text{Am}) \times (\text{Vp}/\text{Vu}) \times 1/\text{w} \quad (1)$$

with N is being the number of specimens counted, Ab the area of used beaker (6079 mm^2), Am the area measured in mm^2 , Vp the volume of residue prepared in mL, Vu the volume used in mL and w the weight of the dry sediment in gram.

Accumulation rates of diatoms and radiolarians were calculated by multiplying abundance values with the shipboard measured dry bulk densities and the linear sedimentation rates (LSR). The LSR values applied are based on updated age models for the targeted sites. A comprehensive overview of these revised age models is available in (Rodrigues de Faria et al., 2024). The models can also be accessed via the Neptune Database (Renaudie et al., 2020, 2023).

2.3 Diatom abundance and diversity

Our study also examines the relationship between diatom diversity and total diatom abundance, which is essential for understanding the influence of diversity on overall community productivity in diatoms. Rather than relying on bulk opal accumulation rates, which do not distinguish the relative contribution of different siliceous groups like radiolarians, we focused on diatom-specific abundance values. This approach provides a clearer understanding of the relationship between diversity and abundance within diatom communities.

To explore these interactions, we compared recent diatom diversity reconstructions (Özen et al., subm.) with diatom abundance data obtained in this study across the E/O transition. This approach allowed us to directly examine how variations in diatom diversity correspond to changes in abundance and to explore the potential implications of these interactions for overall diatom productivity. In our comparisons, by focusing on diatom abundances per gram of sediment,

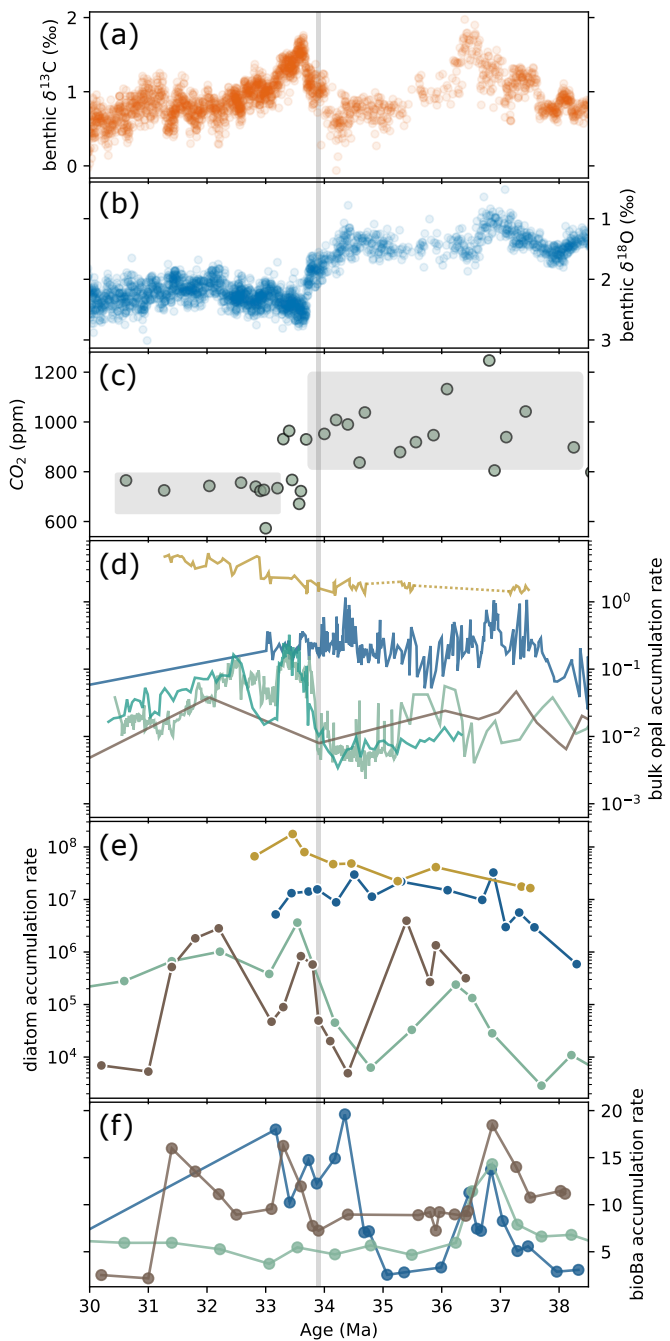
we aimed to minimize potential biases associated with accumulation rates, which can be affected by uncertainties in age models. This approach ensures a more accurate representation of the abundance-diversity relationship, offering valuable insights into the ecological and environmental factors that influenced diatom productivity during the E/O transition.

255 3 Results

Our diatom MARs reveal a prominent clear latitudinal organization in the late Eocene SO, which is expected, as diatoms are a major contributor of biogenic sedimentation at sub-Antarctic sites, the DSDP Site 511 (Falkland Plateau) and ODP site 1090 (Agulhas Ridge) sediments, where biogenic silica is the main sedimentary component across the study interval (Renaudie, 2016; Wade et al., 2020; see Fig. S1).

260

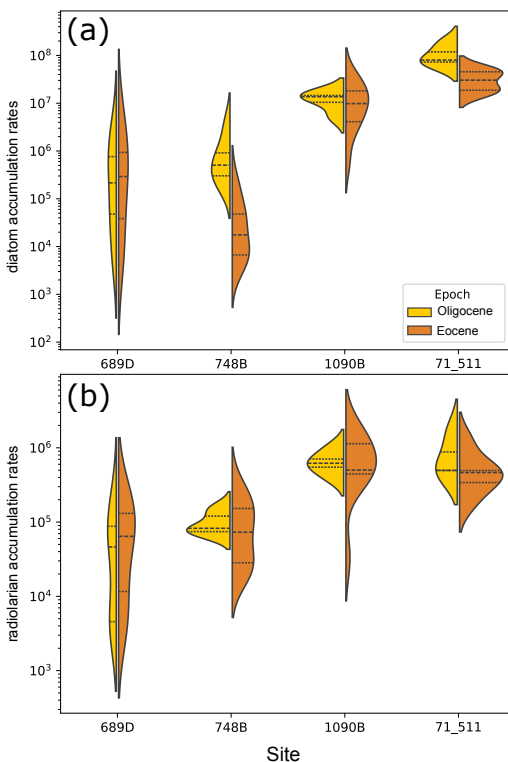
In the sub-Antarctic Atlantic, diatom MARs at ODP Site 1090 diatom MAR increased show an increasing trend from ~38 Ma onward, peaking at around 36.8 Ma, in good agreement with closely matching previously published bulk opal MARs (Diekmann et al., 2004; Anderson and Delaney, 2005, see Fig. 2d and 2e). Site 1090 had an average diatom MAR of 1.26×10^7 frustules/cm²/kyr (with standard deviation (std dev.) 9.48×10^6 , ranging from 5.88×10^5 to 3.26×10^7 . The total 265 number of samples (N) = 15). At DSDP Site 511, diatom MARs gradually rose throughout the late Eocene, peaking near 33.4 Ma (1.76×10^8 , see Fig. 2e), with notably higher accumulation rates (mean = $5.73 \times 10^7 \pm 4.97 \times 10^7$; range: 1.65×10^7 – 1.77×10^8 , N = 9). The overall diatom MAR trends at this site align well with recent bulk opal 270 accumulation rates (Brylka et al., 2024, Fig. 2d). Fig. 3a shows the distributional characteristics of diatom MARs at both sites. Meanwhile, DSDP Site 511 records the highest diatom MARs, with a gradual increase throughout the late Eocene, culminating at around 33.4 Ma (Fig 2d). Our increasing trend across the late Eocene, peaking at ~33.4 Ma (Fig. 2d). Notably, our diatom MAR trend from DSDP Site 511 closely aligns with recently published bulk opal accumulation rates (Brylka et al., 2024, Fig. 2d)



275 **Figure 2.** (a) Global composite benthic foraminiferal $\delta^{13}\text{C}$ and (b) $\delta^{18}\text{O}$ records (from Westerhold et al., 2020). (c) CO_2 compilation (from Zhang et al., 2013; Anagnostou et al., 2020). (d) Diatom mass accumulation rates (MARs) (diatom $\text{cm}^{-2} \text{kyr}^{-1}$, scatter points with solid lines; this study) and Bulk opal accumulation rates ($\text{gr cm}^{-2} \text{kyr}^{-1}$, solid lines) from DSDP 511 (yellow, Brylka et al., 2024), ODP 1090 (blue, Diekmann et al., 2004; Anderson and Delaney 2005), Kerguelen Plateau ODP Sites (light green, 744 and 738; dark green 748) (compiled from Ehrmann, 1991; Ehrmann and Mackensen, 1992; Salamy and Zachos, 1999, Brylka et al., 2024), and ODP 689 (Faul and Delaney, 2010). (e) Diatom mass accumulation rates (MARs) (diatom $\text{cm}^{-2} \text{kyr}^{-1}$, scatter points with solid lines; this study) and Bulk opal accumulation rates ($\text{gr cm}^{-2} \text{kyr}^{-1}$, solid lines) from DSDP 511 (yellow, Brylka et al., 2024), ODP 1090 (blue, Diekmann et al., 2004; Anderson and Delaney 2005), Kerguelen Plateau ODP Sites (light green, 744 and 738; dark green 748) (compiled from Ehrmann, 1991; Ehrmann and Mackensen, 1992; Salamy and Zachos, 1999, Brylka et al., 2024), and ODP 689 (Faul and Delaney, 2010). (f) Diatom mass accumulation rates (MARs) (diatom $\text{cm}^{-2} \text{kyr}^{-1}$, scatter points with solid lines; this study) and Bulk opal accumulation rates ($\text{gr cm}^{-2} \text{kyr}^{-1}$, solid lines) from DSDP 511 (yellow, Brylka et al., 2024), ODP 1090 (blue, Diekmann et al., 2004; Anderson and Delaney 2005), Kerguelen Plateau ODP Sites (light green, 744 and 738; dark green 748) (compiled from Ehrmann, 1991; Ehrmann and Mackensen, 1992; Salamy and Zachos, 1999, Brylka et al., 2024), and ODP 689 (Faul and Delaney, 2010).

solid lines; this study) and (ef) Bbiogenic barium (bioBa) accumulation rates ($\mu\text{mol cm}^{-2} \text{kyr}^{-1}$) from ODP Sites 1090, 689, and 748 (from Rodrigues de Faria et al., 2024).

In the Antarctic sites, showed lower and more variable diatom MARs (Fig. 2e and 3a). Adiatom MARs at ODP Site 689 (Maud Rise), diatom MAR exhibited prominent peaks (within the temporal precision of our data) – fluctuate across the E/O transition, with distinctive peaks at ~ 35.5 Ma, 33.6 Ma, and 32.3 Ma, with an average value of 7.92×10^5 frustules/cm 2 /kyr (std dev. is 1.16×10^6 , range: $4.92 \times 10^3 - 3.94 \times 10^6$, N = 16; see Fig. 2e). At In the Indian Ocean sector, at ODP Site 748 (Kerguelen Plateau), diatom and bulk opal MARs are in agreement after ~ 37.5 Ma, suggesting increasing diatom contribution to the total opal productivity towards the E/O boundary. Mean diatom MAR at this site is 3.74×10^5 , with minimum and maximum values of 2.86×10^3 and 3.63×10^6 , respectively (N = 18). At this site, it has been shown that across the middle Eocene, other siliceous groups, ebridians and radiolarians, dominate the record (Witkowski et al., 2012). Combined with our results, this suggest that diatom dominance in the Kerguelen Plateau region started in towards 37 Ma, which is consistent with our sample surveys that there is a strong presence of ebridians in our samples preceding ~ 38 Ma (See Supplementary Data 1). Moreover, our results show that, compared to the other sites, diatom MAR at ODP Site 748B changed substantially between Eocene and Oligocene (Fig. 3a), with a mean of 4.8×10^4 frustules/cm 2 /kyr in the Eocene and 1.03 in the Oligocene.



300 **Figure 3. Distribution of MARs (specimen cm⁻² kyr⁻¹; in log scale) for (a) diatoms and (b) radiolarians at each studied site (x-axis).** Eocene and Oligocene samples are shown separately (see legend). Lines within each distribution indicate the quartiles, marking the median, the 25th and 75th percentiles.

Our diatom MARs, combined with published bulk opal MAR records, reveal two distinct intervals during the EOT, 36.5–35.5 Ma and 34–33 Ma, when opal productivity at Antarctic sites (ODP 689 and 748) sharply increased, surged to levels approaching those of the sub-Antarctic Atlantic levels (Fig. 2d and 2e). Although sub-Antarctic sites (DSDP 511 and ODP 1090) maintained consistently higher opal productivity throughout the EOT, the Antarctic sites experienced transient but significant increase in diatom MARs during these intervals. These Antarctic productivity peaks temporally, bringing opal flux levels closer to those observed at sub-Antarctic sites narrowed the gap between the two regions.

310 **Crucially, t**These intervals, of Antarctic and sub-Antarctic diatom MAR convergences, unfolded under distinct climatic conditions. The first (~36.5–35.5 Ma) interval broadly aligns coincided with the late Eocene warming event, which has been documented at multiple high-latitude SOuthern Ocean sites (ODP Site 689 (Maud Rise); ODP Sites 738, 744, 748 (Kerguelen Plateau); DSDP Site 277; (Diester-Haass and Zahn, 1996; Bohaty and Zachos, 2003; Villa et al., 2008, 2014; Pascher et al., 2015). In contrast, the later interval (~34–33 Ma) broadly concomitantly or responds with a sharp increase in global foraminiferal $\delta^{18}\text{O}$ in the earliest Oligocene, signalling substantial cooling and the onset of permanent Antarctic glaciation (Fig. 2b and 2d). Although diatom MAR at Antarctic sites temporarily approached sub-Antarctic levels during both intervals, the associated environmental conditions differed markedly.

320 ~~This contrast, where diatom MARs at Antarctic sites surged under opposing climatic regimes, highlights that although Antarctic productivity temporally approached sub-Antarctic levels, these shifts occurred during fundamentally different environmental contexts.~~

325 Radiolarian MAR patterns are broadly in agreement with diatom MARs across the E/O transition, derived from the same samples (Fig. 4c). ~~Our results are summarized in Fig. 3.~~ At ODP Site 1090, ~~our~~ radiolarian MARs ~~revealed~~ showed two prominent peaks at ~37 and 34.5 Ma. The mean accumulation rate at this site is 7.43×10^5 radiolaria/cm²/kyr ($\pm 4.56 \times 10^5$, range: 3.29×10^4 – 1.60×10^6). At DSDP Site 511, ~~diatom~~ MAR values ~~remained relatively stable throughout the late Eocene, exhibiting significant increases towards and after the E/O boundary, at approximately 34 Ma and 33.5 Ma (mean = $6.34 \times 10^5 \pm 4.53 \times 10^5$, range: 1.79×10^5 – 1.56×10^6).~~ do not show any substantial change across the Eocene samples until the E/O boundary. Following the E/O boundary, radiolarian MARs reveal two substantial peaks at ~34.2 and ~33.5 Ma.

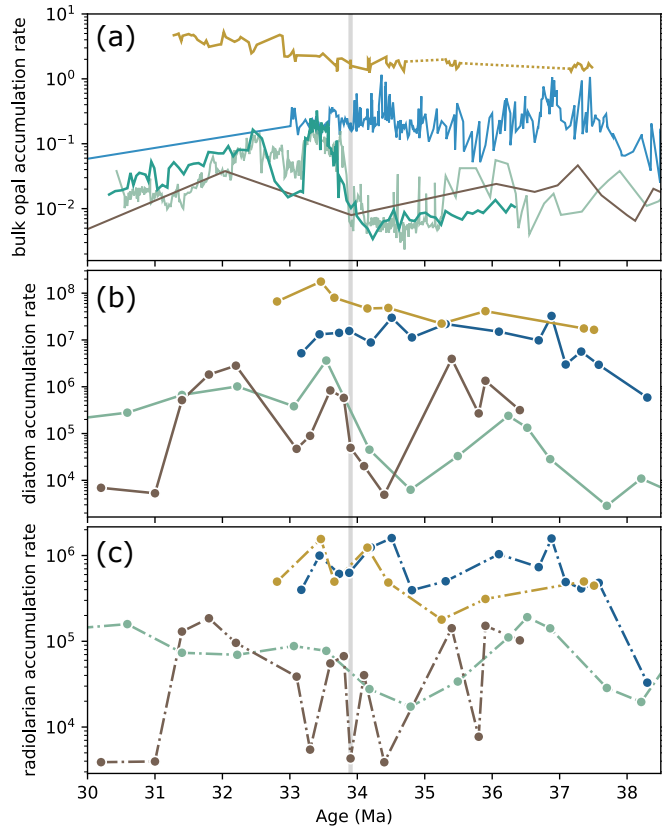
330 At ODP Site 748, ~~the major~~ radiolarian MAR peaked ~~occurs notably~~ at ~36.5 Ma, followed by a ~~significant drop~~ substantial decline, and recovered to pre-E/O levels only around 30.5 Ma (mean = $1.01 \times 10^5 \pm 7.61 \times 10^4$, range: 1.73×10^4 – $3.06 \times$

335 10⁵). Our results suggest that the radiolarian MAR values, ODP 748, recover back to the pre-E/O values only at around 30.5 Ma. Values for ODP site 689 indicated two prominent peaks, between 36–35 Ma, and at ~31.5 Ma, with a lower average MAR of 6.49×10^4 ($\pm 6.20 \times 10^4$, range: 3.89×10^3 – 1.85×10^5). Interestingly, our results reveal that the difference between sub-Antarctic Atlantic and Antarctic sites in radiolarian MARs significantly elevated at approximately 35 Ma onwards. From ~35 Ma onward, radiolarian MAR differences between sub-Antarctic Atlantic (sites 1090 and 511) and Antarctic (sites 689 and 748) sites became more pronounced, reflecting an increasing contrast in accumulation rates during the latest Eocene – early Oligocene (Fig. 4c; see also Fig. S2).

340 | **3.1 Correlation of opal abundance to other paleoproductivity proxies**

Our diatom MARs results reveal a significant overall shift in SO productivity dynamics at approximately around 37 Ma. This is reorganization in SO productivity is not restricted to diatom and radiolarian MARs. Notably, in a recent study based on bio-Ba proxy, it has been shown that there was a strikingly correlated increase in productivity at the ODP Sites 1090, 748, and 689 (Fig. 2e) (Rodrigues de Faria et al., 2024), aligning with the trends observed in our diatom MAR results at ODP site 1090. Although our diatom MAR values do not show great agreement with those seen in bio-Ba values at ODP 748, prominent change in bio-Ba values clearly marks the beginning of the increasing diatom MARs values, peaking at around 36.2 Ma at this site. It has been also shown that, based on benthic foraminiferal accumulation rates (BFAR), at ODP 689, there was a distinct increase in productivity across the 37–36.5 Ma interval (Fig. S2). This interval also marks a significant change in abundance and diversity of the radiolarian communities in the Southern Pacific (Pascher et al., 2015), and in the Antarctic Atlantic (Funakawa and Nishi, 2008). Moreover, in the Kerguelen Plateau region towards 37 Ma, a reorganization in nannofossil assemblages suggesting a substantial eutrophication was documented (Villa et al., 2014) (Fig. S3). These findings, based on multiple productivity proxies, are strikingly consistent with our diatom and radiolarian and strengthen the evidence for a pronounced productivity change and diatom dominance in the SO towards and onwards ~37 Ma.

355 |



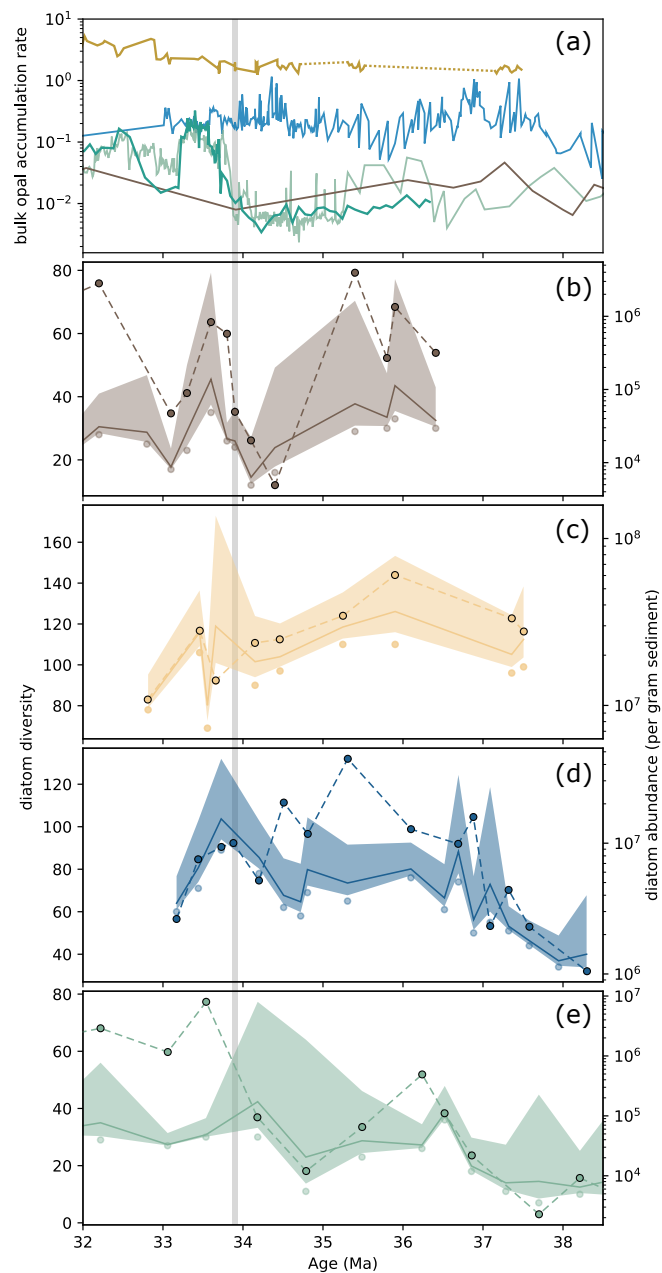
360 Figure 34. Radiolarian accumulation rates (radiolarian $\text{cm}^{-2} \text{kyr}^{-1}$) at the study sites (this study). Comparison of (a) bulk opal, (b) diatom, and (c) radiolarian accumulation rates (specimen $\text{cm}^{-2} \text{kyr}^{-1}$) at SO sites. Site colors are consistent across figures. Diatom and radiolarian data are from this study, while bulk opal accumulation rates (a; $\text{g cm}^{-2} \text{kyr}^{-1}$, solid lines) are compiled from the following sources: DSDP 511 (yellow; Brylka et al., 2024), ODP 1090 (blue; Diekmann et al., 2004; Anderson and Delaney, 2005), Kerguelen Plateau sites ODP 744 and 738 (light green) and ODP 748 (dark green) (Ehrmann, 1991; Ehrmann and Mackensen, 1992; Salamy and Zachos, 1999; Brylka et al., 2024), and ODP 689 (Faul and Delaney, 2010).

365

3.2.1 Correlations between diatom diversity and abundance

370 Diatom abundance and diversity showed varied correlations among sites across the late Eocene – early Oligocene interval (Fig. S3). At DSDP Site 511, exhibiting the highest species diversity, diatom abundance and diversity were in great agreement across the E/O transition (Fig. 4c; see also Fig. S3). At ODP Site 1090, diatom abundance and diversity were generally synchronous in trends, except a clear divergence between approximately 37 and 34.5 Ma, during which diversity values stayed relatively low and constant while abundance values showed the highest values. Moreover, the pronounced peaks in diatom abundance around 36.8 and 34.5 Ma did not correspond with similar increase or trend shift in diatom diversity (Fig. 4d). In contrast, at ODP Sites 689 and 748, diatom diversity and abundance values were in agreement (Fig. 4b and 4e; Fig. S3). At ODP Site 748, there was a substantial increase in both bulk opal (Brylka et al., 2024, Fig. 4a) and

375 diatom abundance, reaching values similar to those seen at sun-Antarctic Atlantic sites ODP 1090 and DSDP 511. However, diversity values remained significantly lower compared to those documented at the sub-Antarctic Atlantic sites (Fig. 45e).



380 **Figure 45.** Comparison of bulk opal accumulation rates ($\text{gr cm}^{-2} \text{ kyr}^{-1}$) with diatom diversity (number of species) and abundance. (a) from DSDP 511 (yellow, Brylka et al., 2024), ODP 1090 (blue, Diekmann et al., 2004; Anderson and Delaney, 2005), Kerguelen Plateau ODP Sites (light green, 744 and 738; dark green 748) (compiled from Ehrmann 1991; Ehrmann and Mackensen 1992;

385 Salamy and Zachos, 1999³⁵ Brylka et al., 2024), and ODP 689 (brown, Faul and Delaney, 2010) (b-e) Diatom diversity (scatter points) with Chao1 diversity estimates (solid line, 95% confidence envelope) (Özen et al., subm.) and diatom abundance per gram sediment (scatter points, dashed lines).

4 Discussion

4.1 Diatom and radiolarian productivity and opal record across the middle-to-late Eocene transition (~36–38 Ma)

390 Although the ~~exact~~ timing and mode of opal productivity (~~that is, the relative contribution of diatoms and radiolarians, the underlying diatom diversity, and whether the flux is pulsed or gradual~~) patterns differ ~~across the~~ ~~among~~ ~~studied~~ sites, our results suggest a substantial reorganization of ~~that~~ SO diatom and radiolarian productivity ~~experienced~~ ~~substantial reorganization~~ between ~36–38 and 36 Ma. In the sub-Antarctic Atlantic, bulk opal ~~records~~ at ODP Site 1090 shows a gradual ~~increase~~ 38 Ma onwards, intensifying by ~37 Ma (Diekmann et al., 2004; Anderson and Delaney, 2005). Our diatom MARs ~~from this site~~ ~~greatly agree with~~ closely follow this trend, suggesting increasing ~~growing~~ diatom dominance in the region.

395 This shift ~~in SO productivity~~ was not confined to a single site or proxy but occurred ~~reflects~~ a broader reorganization across multiple ~~oceanic~~ sectors: ~~–~~ during the middle to late Eocene transition. In the Southern Pacific, radiolarian communities in the South Pacific ~~underwent restructuring~~ reorganized (Pascher et al., 2015). In the Indian Ocean sector, and in the Indian Ocean sector both bulk opal and diatom MARs rise between ~38–36 Ma (Fig. 2 d-e, ODP 748 and 400 744), in parallel with evidence for increasing eutrophic conditions from calcareous nannofossil assemblages ~~also show~~ significant changes (Villa et al., 2014, see Fig. S1), alongside a surge in biological barium (bioBa) accumulation rates (Rodrigues de Faria et al., 2024, Fig. 2e), indicating increased export productivity (Villa et al., 2014, see Fig. S4), confirming that the diatom signal reflects a real productivity shift.

405 In the Atlantic sector, benthic foraminiferal accumulation rates (Diester-Haass and Zahn, 1996, see Fig. S5) and radiolarian communities (Funakawa and Nishi, 2008) record this shift in productivity and environmental conditions. Bio-Ba records from ODP Sites 1090, 689, and 748 (Rodrigues de Faria et al., 2024) document a ~37 Ma export productivity peak that is synchronous with the diatom MAR rise at ODP Site 1090 but leads peaks at Antarctic-adjacent sites (ODP 689, 748) by ~0.5–1 Myr (Fig. 2e). This offset does not reflect differences in age models, as 410 identical samples and age models were used in both datasets, and likely reflects regional environmental controls during middle-to-late Eocene, including latitudinal differences in sea-surface temperature (e.g., Douglas et al., 2014; Sauermilch et al., 2021), variations in nutrient distribution, and circulation patterns influenced by still-shallow SO gateways (e.g., Sauermilch et al., 2021; Rodrigues de Faria et al., 2024). Similar productivity reorganizations are evident in the Atlantic sector, where benthic foraminiferal accumulation rates (BFAR) exhibit a substantial increase 415 (Diester-Haass and Zahn, 1996, see Fig. S2). Moreover, comparable opal productivity surges around this time

interval have been documented in the equatorial (Nilsen et al., 2003, see Fig. S3), and northern Atlantic (Witkowski et al. 2021), suggesting that the changes across the middle-to-late Eocene transition may have been regionally widespread within the Atlantic basin.

420 An increase in productivity at ~37 Ma has been documented across SO ODP Sites 1090, 689, and 748 based on bioBa records (Rodrigues de Faria et al., 2024, Fig. 2e). Our diatom MARs at ODP Site 1090 align well with this trend but at Antarctic adjacent sites, ODP 689 and 748, diatom productivity peaks within ~36–35.5 Ma (Fig. 2d), indicating a temporal lag between bioBa and diatom accumulation at these sites. This asynchrony suggest that diatom productivity did not increase uniformly across sub-Antarctic Atlantic and Antarctic adjacent regions and may have been influenced by regional environmental factors and/or differential plankton community composition across the SO regions. Such dominant plankton community variability is consistent with diatoms as *relative newcomers*, gradually expanding their ecological role within an ecosystem previously dominated by other plankton groups, such as calcareous nannoplankton.

430 What does this productivity reorganization across the middle-to-late Eocene transition (~38–36 Ma) signify? It encompasses a suspected ephemeral East Antarctic glaciation, namely Priabonian Oxygen Maximum (PrOM, ~37 Ma; Scher et al., 2014). This event is marked by a sharp negative Neodymium (Nd) excursion within a broader late Eocene positive trend (Scher and Martin, 2006; Scher et al., 2014; Wright et al., 2018). Previous studies link PrOM cooling to productivity shifts across SO sectors (e.g., Villa et al., 2014; Pascher et al., 2015; Rodrigues de Faria et al., 435 2024) through mechanisms involving transient intensification and organization of a proto-ACC that enhanced frontal upwelling and nutrient delivery (e.g., Rodrigues de Faria et al., 2024). This interpretation is consistent with modelling results suggesting that even a shallow opening of the Drake Passage, which likely during the late middle-Eocene (Scher and Martin, 2004; 2006), could have reorganized ocean flow and promoted proto-ACC formation (Toumoulin et al., 2020). A comparable mechanism operates in the modern SO, where the strength of the latitudinal temperature gradient controls westerly wind intensity, which governs ACC transport and the intensity of wind-driven upwelling (R. Rintoul et al., 2001). In parallel, PrOM cooling, in line with southern high-latitude SST compilations (O'Brian et al., 2020), would have steepened the temperature gradient, intensified the westerlies that drive proto-ACC, and increased Ekman divergence, delivering nutrient-rich waters to the surface ocean. Silicon isotope data further support this scenario, indicating increased diatom silicic acid utilization during this interval and pointing to enhanced silicic acid supply to surface ocean via intensified upwelling (Egan et al., 2013). Consistent with this, although site 440 level responses vary, diatom and radiolarian accumulation rates between 38 and 36 Ma show positive covariation at Agulhas Ridge and the Kerguelen Plateau. This pattern is more consistent with a shared physical driver, enhanced upwelling and nutrient supply, than with competitive replacement under constant nutrient conditions.

450 We note that, in addition to diatoms and radiolarians, other sources of biogenic silica, such as sponge spicules, silicoflagellates and ebridians, can also contribute to bulk opal, which may complicate direct comparisons with group-specific records. In our samples, these groups are not a significant component. Our focus therefore remains on diatoms and radiolarians to assess how their contributions changed through time within the broader biogenic silica pool, rather than attempting a one-to-one correspondence with bulk opal records.

455 Viewed in broader context, these productivity changes in plankton diatom and radiolarian record productivity (as summarized above) and community composition (e.g., Pascher et al., 2015; Özen et al., subm.) across the middle-to-late Eocene transition (~36–38 Ma) (e.g., Pascher et al., 2015; Özen et al., subm.) are interpreted here as a response to increasing SO circulation and associated enhancements in nutrient distribution and upwelling. At the same time, this transition marks the onset of global rise in diatom abundance and diversity (Renaudie et al., 2016), and in our records diatom MARs show a net increase at all sites except ODP 689 during the subsequent interval, pointing to a basin-wide reorganization of diatom export. Indeed, comparable opal productivity surges during ~38–36 Ma are recorded in the equatorial Atlantic (Nilsen et al., 2003; Fig. S6) and northern Atlantic (Witkowski et al., 2021), suggesting that reorganization had a broad geographic reach and may reflect the strengthening of a cross-latitudinal circulation system enhanced nutrient distribution across the Atlantic, hinting at an invigorated cross-latitudinal circulation system, akin to the modern Atlantic Meridional Ocean Circulation (AMOC). Indeed, it has been proposed that ~38 Ma onwards this circulation started to strengthen under the effect of increasing circum-Antarctic circulation, often termed as the proto-ACC, which is an integral part of the cross-latitudinal circulation across the Atlantic (Borrelli et al., 2014). This aligns with our diatom accumulation rates, which show a substantial reorganization 38 Ma onwards, aligning with earlier and as well as with the previous paleoproductivity reconstructions suggesting a substantial productivity increase across the SO sites between 36–38 Ma (e.g., Diester-Haass and Zahn, 1996; Pascher et al., 2015; Rodrigues de Faria et al., 2024). Although the precise timing and sequence of SO gateway opening However, there are numerous controversies on evolution and steps of the development of circum-Antarctic Atlantic circulation patterns remain debated (Diester-Haass and Zahn, 1996; Mackensen, 2004; Stickley et al., 2004; Scher and Martin, 2006; Livermore et al., 2007; Barker et al., 2007; Hodel et al., 2021; Evangelinos et al., 2024), despite the divergent accounts of the opening and deepening of the SO gateways, the balance of evidence suggests a system of circulation which got started to late Eocene strengthening of circum-Antarctic circulation in the late Eocene, possibly during the middle-to-late-Eocene transition, that set the stage for a large-scale reorganization of SO productivity and the growing dominance of diatoms.

480 Interestingly, ~37 Ma also marks a suspected ephemeral east Antarctic glaciations, named as the Priabonian Oxygen Maximum event (PrOM) (Scher et al., 2014). This event is marked by a sharp negative excursion in Neodymium (Nd) values, superimposed on a broader positive Nd trend observed throughout the late Eocene (Rodrigues de Faria et al., 2024, after Scher and Martin, 2004, 2006; Scher et al., 2014; Wright et al., 2018). While the overall positive trend in Nd values has

been interpreted as evidence for an increasing Pacific influence into the Atlantic sector the SO, likely through Drake Passage 485 widening (Seher and Martin 2004; Rodrigues de Faria et al. 2024), the substantial negative excursion at ~37 Ma, as a stark contrast to the overall positive trend across the late Eocene, has been attributed to glacial weathering discharge into the Kerguelen Plateau region, associated with the PrOM event (Seher et al., 2014).

The PrOM (~37 Ma) event coincides with significant changes in productivity in the Kerguelen Plateau region (Villa et al. 490 2014; Rodrigues de Faria et al., 2024), suggesting enhanced glacial weathering discharge may have supplied key nutrients, fueling productivity in the Indian Ocean sector of the SO. However, our diatom MAR results, and bulk opal data do not indicate a strong link between PrOM event and opal productivity. Notably, the link between negative Nd excursion (data 495 from Seher et al. 2011) and opal productivity is particularly striking in the earliest Oligocene (Fig. S4), where their strong correlation suggests that glacially modulated weathering discharge, as short lived negative Nd excursions suggest (Seher et al., 2011), may have directly influenced nutrient availability and biological productivity in the region. The link between the PrOM and the late Eocene pulse needs however to be addressed in further studies.

The opal pulse across the middle to late Eocene is also unique as it marks not simply abundance increase in both diatoms 500 and radiolarians, but also a substantial reorganization in diatom communities. It has been shown that towards 37 Ma there is an accompanying increase in diatom diversity (Özen et al., subm.). Although this apparent diversity increase can be simply a function of the increasing abundance and/or preservation of diatoms, the observation that community composition was dynamically changing with the climate suggest that invigorated circulation system possibly led to increasing nutrient availability in our targeted regions, and this paved the way to increasing carrying capacity and available niches for the more diverse communities. Moreover, within the same timeframe, community changes are not restricted with diatoms, it has been 505 shown that radiolarian communities experienced such re-organization too (Funakawa and Nishi, 2008; Pascher et al., 2015). We detail diatom abundance/diversity relation in the Section 4.5 Diatom diversity and productivity: a cause-effect relation?

4.2 Opal pulse across at the E/O boundary

Two overarching patterns characterize SO productivity across the E/O boundary (~35.5–32 Ma): (1) strong regional 510 heterogeneity (see Brylka et al., 2024; Rodrigues De Faria et al., 2024), and (2) distinct latitudinal responses. During the latest Eocene, diatom and radiolarian MARs diverge between sub-Antarctic (DSDP 511; ODP 1090) and Antarctic sites (ODP 689; ODP 748). At the Antarctic sites, both groups decline (Fig 4b-c), consistent with low bulk-opal values on the Kerguelen Plateau and bio-Ba signals (Fig. 2d and 2f). In contrast, sub-Antarctic records show high latest-Eocene productivity: bulk opal, diatom MARs, and bio-Ba peak near ~34.5 Ma, especially at Agulhas Ridge (ODP 1090), while the Falkland Plateau (DSDP 511) maintains high diatom productivity (see Fig 2d-e).

515 It is now well established from a variety of studies, that the E/O boundary marks a substantial increase in opal productivity in the SO. This is the second pulse of productivity across the E/O transition, which is the most pronounced in the Antarctic

ODP Sites 689 and 748 where our results suggest approximately 100-fold increase, suggesting a stark dominance of diatoms in the Antarctic sites, where radiolarian abundance particularly low (Fig. 3, see Discussion section 4.4. Environmental implications of radiolarian MARs).

520 Latitudinal divergence between sub-Antarctic and Antarctic sites strengthens from ~35.5 Ma onward (Fig. 4a-c; Fig. S2). This divergence is also evident in radiolarian productivity: before ~35.5 Ma, radiolarian MARs co-vary between the two regions, but from 35.5 Ma onward they diverge, signalling a change in biogeography and productivity. Indeed, radiolarian endemism in the southern high latitudes rises from ~35.5 Ma (Lazarus et al., 2008), consistent with greater regional isolation or reorganization of water masses. Tectonic reconstructions point to further

525 Tasmanian Gateway (TG) deepening at about the same time (Stickley et al., 2004), although Nd-isotope data imply that fully developed deep throughflow likely did not establish until the Neogene (Evangelinos et al., 2022). A step-like increase in the negative Ce anomaly at ~35.5 Ma indicates increased oxygenation of thermocline and bottom waters in the SW Pacific (Hodel et al., 2022), and the authors link this change to TG tectonic evolution and enhanced vertical mixing. Against this background circulation change, the Kerguelen Plateau region records a gradual ecological

530 transition from a radiolarian-dominated to a diatom-dominated phase (Fig S7). This shift occurs while overall opal flux remains low in the Antarctic-adjacent sites, pointing to altered competitive balance between siliceous plankton rather than a simple increase in nutrient supply. Broader confirmation of circulation reorganization comes from dinocyst biogeography and sedimentological evidence, which record stronger SO circulation and surface cooling from ~35.7 Ma (Houben et al., 2019).

535 Taken together, these lines of evidence indicate that circum-Antarctic circulation, which had already begun to strengthen across the middle-to-late Eocene transition, underwent further intensification from ~35.5 Ma. We interpret this reinforcement of circulation and vertical mixing as the main driver of the growing divergence between sub-Antarctic and Antarctic sites. Model simulations are consistent with this view: experiments with late-Eocene

540 boundary conditions show that progressive gateway deepening enhanced eastward circumpolar flow, reorganized upper-ocean circulation, and shifted deep-convection zones northward toward ~40 °S, encapsulated the Agulhas Ridge region (Toumoulin et al., 2020). This circulation shift has indeed been linked to substantial export productivity at ODP Site 1090 in the latest Eocene (Rodrigues De Faria et al., 2024; Fig. 2f), which possibly also underlies the opal productivity burst and overall high diatom productivity we observe at this site (Fig. 2d-e). At the same time, this

545 northward shift of deep-convection would have reduced circulation strength in Antarctic-proximal sectors, particularly the Weddel region (see Toumoulin et al., 2020), which in turn would have reduced upwelling, nutrient supply, and export production (Rodrigues De Faria et al., 2024). The combined effect of a further strengthening proto-ACC and a weakened Antarctic circulation system offers a plausible mechanism for the sustained decline in diatom and radiolarian productivity at Antarctic sites from ~35.5 Ma to the E/O boundary.

555 In Antarctic-adjacent sites, the latest Eocene low-productivity regime shifts at the E/O boundary. Diatom MARs rise sharply, closely matching bulk-opal accumulation (Fig. 2d) and coinciding with the largest increase in global $\delta^{18}\text{O}$ values (Fig. 2b), suggesting a link between the East Antarctic glaciation, cooling, and enhanced diatom productivity.
560 Clay-assemblage studies suggest stronger physical weathering in the earliest Oligocene at Maud Rise (ODP 689) and the Kerguelen Plateau (ODP 748) (Robert et al., 2002). Such weathering likely increased silica input and fueled higher productivity in these regions. Consistently, the earliest-Oligocene Nd-isotope excursion in the Kerguelen Plateau, tied to glaciation and weathering (Scher et al., 2011), strongly correlates with opal flux (see Fig. S8), reinforcing the link between continental discharge and silica supply. In contrast, radiolarian productivity does not return to early late-Eocene levels (Fig. 4c). Instead, it remains low while diatoms increase strongly, suggesting that diatoms progressively gained dominance, likely reflecting their competitive advantage in utilizing the available silicic acid.

565 We note that geographically variable diatom flux across SO sites may not necessarily imply regionally inconsistent forcing. Sub-Antarctic sites supported diverse diatom communities (see Section 4.3) and already sustained high fluxes in the late Eocene, likely operating close to ecological carrying capacity, which may have muted the magnitude of their response. The biological basis for such a ceiling is well captured by the relationship between abundance and silicic acid in coastal upwelling zones: sedimentary diatom abundance increases as silicic acid concentrations rise until a threshold is reached, beyond which further silicic acid input yields little additional diatom accumulation (Abrantes et al., 2016). This diminishing return complicates efforts to trace a coherent sequence of diatom
570 productivity and oceanographic reorganization across the SO, because increased silica supply via upwelling in already productivity sub-Antarctic regions, such as DSDP 511 and ODP 1090, may have altered community composition or frustule silicification rather than producing a proportional increase in diatom productivity and thus opal flux.

575 At Antarctic adjacent ODP Sites 689 and 748, the substantial increase in diatom MARs aligns closely with bulk-opal accumulation rates (Fig. 2d) and coincides with the largest shift in global $\delta^{18}\text{O}$ values, suggesting a link between the emplacement of permanent East Antarctic glaciation, global cooling and opal productivity. Additionally, clay assemblage studies indicate an increase in physical weathering regime in the earliest Oligocene at both Maud Rise (ODP 689) and Kerguelen Plateau (ODP 748) regions (e.g., Robert et al., 2002). This is consistent with the scenario that enhanced weathering influx may have contributed to increase silica availability, fueling opal productivity in Antarctic adjacent regions (ODP 689 and 748) during the earliest Oligocene. Moreover, the earliest Oligocene Nd excursion shows a strong correlation with opal productivity, reinforcing the link between weathering discharge and silica supply (Scher et al., 2011; see previous section, Discussion Section 4.1).

4.3 Transient geographical shifts in diatom productivity

585 Our results, together with previously published bulk opal records, reveal a striking pattern in the SO opal record: two extended intervals, 36.5–35.5 Ma and 34–33 Ma, when diatom productivity at Antarctic sites (ODP 689 and 748) increased substantially, approaching levels typically observed in the sub-Antarctic Atlantic (ODP 1090 and DSDP 511; see Fig. 2d). While the mechanisms underlying such transient geographic shifts are beyond the exact focus of our work, the observed fluctuations between sub-Antarctic Atlantic and Antarctic sites reveal a striking pattern.

590 This apparent latitudinal organization of diatom productivity may reflect the presence of an early frontal system, possibly linked to a developing proto-circum-Antarctic circulation. As Antarctic sites (ODP 689 and 748) show episodic increases in diatom productivity, approaching sub-Antarctic values, this pattern may indicate an early-stage frontal structure influencing nutrient distribution and productivity gradients across the SO. In the modern SO, 595 frontal systems are integral to nutrient distribution and show latitudinal shifts in response to climatic oscillations (e.g., Howard and Prell, 1992; Chapman et al., 2020). This parallel suggests that emerging frontal systems during the late Eocene may have facilitated nutrient redistribution in the SO, directly influencing diatom productivity at high latitudes. Therefore, these apparent geographical shifts could represent an early iteration of the nutrient gradients and productivity shifts observed in the modern SO.

600 4.4 Environmental implications of radiolarian MARs

The late Paleogene Southern Ocean radiolarian communities are an integral part of the silica cycle across the Eocene–Oligocene Transition. Our data indicates a noteworthy latitudinal disparity in radiolarian MARs, particularly evident at the E/O boundary. Sub-Antarctic sites (ODP 1090 and DSDP 511) experienced a significant increase in MAR values, while 605 there was a sharp decline in the Antarctic margin (ODP 689 and 748) (Fig. 3). This latitudinal organization suggest a possible northward shift in locus of maximum radiolarian productivity toward the sub-Antarctic region due to substantial cooling at the Antarctic margin. Alternatively, markedly low radiolarian MARs in the Antarctic margin may reflect the growing dominance of diatom communities in that region, resulting in reducing silica availability for the radiolarian communities.

610 4.53 Diatom diversity and productivity: A cause/effect relation?

One of the most critical defining features of SO opal productivity across the E/O transitions is that it is concurrent its parallel with the substantial major changes in community compositions in both diatom and radiolarian 615 communities community composition (Funakawa and Nishi, 2008; Lazarus et al., 2008; Pascher et al., 2015; Özen et al., subm.). Under the influence of the dynamic climatic and oceanographic features of the SO, and within the precision limits of the fossil data resolution provides, it is a complex task tracking the exact ecological response dynamics of the biosiliceous plankton. The changing diatom community composition and increasing diversity (Özen et al., subm.), is however expected to be positively associated with the range of functional traits within the community (Tréguer et al., 2018), and this to increasing

efficiency in the nutrient utilization which is one of the operating terms for the biological carbon pump efficiency (Farmer et al., 2021).

620 However, ~~The close relationship between observed diversity and diatom MARs and abundance, however, does not necessarily reflect a simple cause-effect link. Observed diversity could increase as a function of abundance through ecological interactions, or it could be an artefact of higher opal flux, better frustule preservation, and thus more morphologies recorded. might simply suggest that observed diversity can be a function of increasing abundance, either by ecologic links as above, or in the other direction of causation: by the links between opal flux, sediment opal abundance, skeletal preservation, and diversity of preserved morphologies.~~ Our findings suggest that while there is a notable correlation between diversity and abundance (see Fig. 45b-e), the ~~directionality of their influence~~relationship is not straightforward, reflecting a more intricate interplay between these two metrics. ~~A~~For instance, at ODP Site 748, ~~for instance, diatom abundance rise sharply in during~~ the earliest Oligocene (Fig. 5e), ~~diatom abundance shows a significant increase~~ (Fig. 4e), yet diversity remains relatively low, barely reaching 30 species. This contrasts with observations at ODP Site 1090, where similar abundance values are associated with much higher diversity, suggesting that abundance alone does not drive diversity (Fig. 5d). Furthermore, at ODP 1090, a period of consistently high diatom abundance between 36.5 and 34.5 Ma corresponds to relatively low and stable diversity ~~values~~, indicating community stability rather than a direct abundance-diversity ~~relationship~~coupling. Notably, this interval at ODP Site 1090 is marked by the dominance of a specific diatom genus, *Pyxilla*, (Özen et al., subm.) which is likely contributed to the observed stability in diversity despite high overall abundance. Interestingly, in the second opal pulse at ODP 1090, diversity declines ~~even as while~~ abundance remains high, further ~~illustrating that questioning the assumption that these two metrics, diversity and abundance~~ need not covary, are ~~directly linked, or that observed diversity is primarily controlled by preservation~~ nor can diversity be reduced to a function of preservation alone.

640 On the other hand, data from DSDP Site 511 ~~for example~~ reveal a strong alignment between diatom abundance and diversity (Fig. 45c). This can be interpreted in an ecologic context, suggesting that the strength of the diversity-abundance relationship ~~between diversity and abundance~~ can vary considerably depending on the site-specific conditions, community composition, and the associated functional groups. Comparable patterns are seen in the modern ocean: metabarcoding surveys indicate that diatom diversity is not uniformly coupled to abundance but instead reflects the balance between a few dominant species and many rare ones, structured by regional circulation and ecological filtering (Malviya et al., 2016). This perspective reinforces the importance of incorporating biological and ecological dimensions into paleoproductivity studies on diatoms, in line with previous work emphasizing the role of community composition in maintaining ecosystem function and the efficiency of carbon export through diatomaceous pathways This variability ~~highlights the critical need to account for local factors and align with previous ecologic studies (e.g., (Tréguer et al., 2018), which emphasized the role of community composition in maintaining ecosystem function and the efficiency of the~~

carbon export through the diatomaceous pathway. It is plausible that diversity and abundance are co-dependent, with external environmental conditions playing a pivotal role in shaping their dynamics. Taken together, our results suggest that the interplay between diatom diversity and abundance is not merely additive, but a feedback loop modulated by external environmental conditions.

655 | 4.64 Diatom productivity and its possible role in the E/O cooling

Studies to date indicate that, across the EOT, SO regions experienced substantial shifts in productivity. Studies to date indicate that, during the late Eocene phase of climatic cooling, SO regions experienced substantial shifts in productivity (e.g., Diester-Haass and Zahn, 1996; Diekmann et al., 2004; Anderson and Delaney, 2005; Egan et al., 2013; Villa et al., 2014; Plancq et al., 2014; Pascher et al., 2015; Rodrigues de Faria et al., 2024). These shifts provide the basis for the hypothesis that increasing productivity may have contributed to declining CO₂ drawdown levels at the end of the Eocene through the biological carbon pump (Salamy and Zachos, 1999; Scher and Martin, 2006; Egan et al., 2013). Our findings add weight to this view: records across the EOT show rising diatom accumulation together with increasing community diversity indicate that increasing diatom accumulation, coupled with the diverse SO diatom communities (Özen et al., subm.), consistent with this a notable feature of the SO productivity system during the late Eocene. This observation aligns with earlier studies using the Si isotope proxy evidence for pulses of silica utilization and associated changes in carbon export (e.g., Egan et al., 2013), which point to diatom-driven and diatom-contributed productivity pulses and associated changes in carbon export into the deep ocean as a potential mechanism contributing to the CO₂ drawdown across the E/O transition. We emphasize, however, that diatom productivity was not an overriding mechanism in itself but one element within a broader climatic and oceanographic mosaic that together shaped CO₂ drawdown across the E/O boundary.

A frequent criticism of a diatom-driven increase in productivity and its potential role in E/O cooling is that opal-rich sediments are restricted to a few regions often focus on the lack of biogenic opal as the dominant sedimentary component outside, for instance, such as the Agulhas Ridge and Falkland Plateau regions (e.g., Wade et al., 2020).

675 However, this argument is largely shaped by sediment classification systems that emphasize the most abundant component and have historically favored carbonate-rich deposits. Several biases contribute to the underrepresentation of biogenic silica in the deep-sea sediment record: (1) a bias towards carbonate pelagic sedimentation due to substantial carbonate rock weathering on land, (2) pelagic primary sediment names based on the most abundant single sedimentary component, and (3) a historical preference in deep-sea drilling for well-preserved carbonate sections, often chosen for 680 geochemical studies. As a result, compilations which rely only on primary dominant sediment types, mostly reflect pelagic carbonates while underestimating the presence of biogenic silica. In contrast, studies using that make use of quantitative estimates of biogenic silica in sediments (e.g., smear slide analyses, Renaudie, 2016) are in principle provide a more accurate, though still incomplete, picture of representation of the history of biogenic silica accumulation. Given

these limitations, the absence of opal-dominated sediments in broad sediment classifications does not contradict the evidence
685 for increased biogenic opal deposition. Indeed, our results ~~consistently~~ show a clear rise in biogenic opal across all targeted sites, providing a robust ~~line of~~ evidence for enhanced diatom productivity across the EOT.

However, the mode and magnitude of the opal deposition/preservation vary between ~~the~~ sites, reflecting local depositional settings and preservation conditions as a natural consequence of the fact that deposition processes in each site is controlled by geologically different settings. Despite these differential geological filters, intervals of productivity reorganization identified in earlier studies are also evident in our records. Importantly, these productivity events coincide with taxonomic shifts in evidence from previous studies, mentioned above, highlight critical intervals during which productivity across the SO sites exhibited substantial reorganization, in agreement with our results. Moreover, recent studies show that the SO productivity events across the E/O transition are interlinked with taxonomic reorganizations within diatom communities (Özen et al., subm.), which changes that may have might tuned the efficiency of the biological carbon pump (Tréguer et al., 2018).

Over and above these, diatoms are particularly efficient effective at the carbon exporters into the deep ocean of organic carbon (Ragueneau et al., 2000; Tréguer et al., 2018). It is known that diatom-dominated export buffers particulate organic carbon (POM) much better than e.g. coccolithophore sourced export against microbial decomposition in the mesopelagic zone far more effectively than coccolithophore-dominated fluxes (e.g., Cabrera-Brufau et al., 2021). The us, the late Eocene increasing in diatom abundance and diversity in diatoms would thus have improved the efficiency of the biological carbon pump, and thus enhancing drawdown of CO₂ drawdown even without a marked rise in total SO productivity. This effect gains further weight considering that Lastly, the Eocene CO₂ levels values proposed for the late Eocene were already close to very near the those proposed as threshold values (~750 ppm) thought necessary for initiating Antarctic ice sheet initiations (DeConto and Pollard, 2003), though we note that such thresholds are model-dependent and vary with boundary conditions (Gasson et al., 2014). Thus, increasing oceanic productivity, and the greater efficiency of enhanced diatom-mediated efficiency of carbon export may have played a role as provided the final touch that in pushing the CO₂ levels below the boundary conditions, and thus contributing to the E/O climate shift.

5 Conclusion

This study focuses on the complex dynamics of diatom productivity and community diversity during across the late Eocene, a period in which the final decline of as the Cenozoic Hothouse took place came to an end and particularly marked in the SO underwent a major productivity reorganization by an opal pulse around form ~3837 Ma onward. Our findings reveal show that this period saw a pronounced marked increase in diatom abundance alongside, coinciding with a major

reorganizations in both diatom (Özen et al., subm.) and radiolarian (Lazarus et al., 2008; Pascher et al., 2015) communities, as well as an overall rise in productivity across the SO productivity (e.g., Diester-Haass and Zahn, 1996; Anderson and Delaney, 2005; Villa et al., 2014; Rodrigues de Faria et al., 2024). These changes point to a broad evolutionary and productivity shift, This suggests a widespread evolutionary and productivity shift likely driven by major changes in ocean circulation, including the early development of the Atlantic Meridional Overturning Circulation (AMOC) (e.g., Borrelli et al., 2014) and the strengthening of the circum-Antarctic currents (e.g., Houben et al., 2019; Sarkar et al., 2019; Rodrigues de Faria et al., 2024).

Bulk opal records content and its accumulation rates are not fully informative metrics for understanding diatom productivity dynamics and its impact on the biological carbon pump and thus atmospheric $p\text{CO}_2$. It is because (1) bulk opal accumulation rates measurements (1) fail to differentiate between contributions from diatoms and other biosiliceous plankton, like such as radiolarians, to the total biogenic silica production and (2) overlook the biological background of productivity, particularly diversity and community composition, which diatom diversity is a critical important contributor to component of diatom-mediated carbon sequestration (Tréguer et al., 2018). Our study integrates both the diversity and abundance dynamics of diatoms across the EOT during the late Eocene, revealing that increases in both the increased abundance and diversity of diatoms likely enhanced the efficiency of the biological carbon pump from across the late Eocene, 38 Ma onwards. This enhancement reflects not only higher diatom abundance but also more effective nutrient utilization linked to diversity, is attributed to both increased abundance of diatoms and more effective nutrient utilization with increasing diversity, which together may have facilitated supported a stronger carbon flux to the ocean interior for a sustained period of time. We therefore highlight SO diatom expansion,

Our observations through both on the synthesis of diatom abundance and increasing diversity, as an important are component of the late Eocene carbon cycling. While the precise strength of the link between diatoms and global cooling across the EOT remains uncertain, our results support the view that diatoms contributed to the efficiency of the biological carbon pump during this critical interval, and that their role deserves continued attention in underestimating the mechanisms behind Cenozoic climate dynamics. particularly significant given the role diatoms play in carbon cycling and export (e.g., Smaleek, 1999). Changes in both the abundance and composition of diatom communities can influence the efficiency of the biological carbon pump (Tréguer et al., 2018), potentially affecting how carbon is sequestered into the deep ocean over long timescales. However, the strength of this connection in the late Paleogene remains uncertain. Nevertheless, as there is no evidence to suggest otherwise for the late Paleogene oceans, our results support the hypothesis that the expansion of diatoms (both in abundance and diversity) during late Eocene could have contributed to shifts in the efficiency of the biological carbon pump, potentially playing a role in the climate trends (e.g., Sigman and Hain, 2012). That is why the mechanistic link between diatom expansion and cooling across the EOT remains a strong conjecture that deserves further investigation.

750 **Data availability**

The supplementary information and raw data are available in the Supplement, and the raw data will be available upon publication on Zenodo (10.5281/zenodo.14826336, Özen et al., 2025).

Supplement

The supplement related to this article is available online at:

755 **Author Contribution**

VÖ collected and analyzed the data and drafted the manuscript. All authors contributed to revision and editing of the final version.

Competing interests

The contact author has declared that none of the authors has any competing interests.

760 **Acknowledgements**

We thank Sylvia Dietze (MfN Berlin) for her assistance with sample preparation.

Financial Support

This study was funded by the Federal Ministry of Education and Research (BMBF) under the “Make our Planet Great Again – German Research Initiative”, grant number 57429681, implemented by the German Academic Exchange Service (DAAD).

765 **References**

[Abrantes, F., Cermeño, P., Lopes, C., Romero, O., Matos, L., Van Iperen, J., Rufino, M., and Magalhães, V.: Diatoms Si Uptake Capacity Drives Carbon Export In Coastal Upwelling Systems, https://doi.org/10.5194/bg-2015-517, 22 February 2016.](#)

770 | Anagnostou, E., John, E. H., Babilia, T. L., Sexton, P. F., Ridgwell, A., Lunt, D. J., Pearson, P. N., Chalk, T. B., Pancost, R. D., and Foster, G. L.: Proxy evidence for state-dependence of climate sensitivity in the Eocene greenhouse, *Nature Communications*, 11, 4436, <https://doi.org/10.1038/s41467-020-17887-x>, 2020.

775 Anderson, L. D. and Delaney, M. L.: Middle Eocene to early Oligocene paleoceanography from Agulhas Ridge, Southern Ocean (Ocean Drilling Program Leg 177, Site 1090): Eocene-Oligocene Paleoceanography, Paleoceanography, 20, <https://doi.org/10.1029/2004PA001043>, 2005.

780 Baldauf, J. G. and Barron, J. A.: Evolution of Biosiliceous Sedimentation Patterns Eocene Through Quaternary: Paleoceanographic Response to Polar Cooling, in: Geological History of the Polar Oceans: Arctic versus Antarctic, edited by: Bleil, U. and Thiede, J., Springer Netherlands, Dordrecht, 575–607, https://doi.org/10.1007/978-94-009-2029-3_32, 1990.

785 Barker, P. F.: Scotia Sea regional tectonic evolution: Implications for mantle flow and palaeocirculation, Earth-Science Reviews, 55, 1–39, [https://doi.org/10.1016/s0012-8252\(01\)00055-1](https://doi.org/10.1016/s0012-8252(01)00055-1), 2001.

790 Barker, P. F., Filippelli, G. M., Florindo, F., Martin, E. E., and Scher, H. D.: Onset and role of the Antarctic Circumpolar Current, Deep Sea Research Part II: Topical Studies in Oceanography, 54, 2388–2398, <https://doi.org/10.1016/j.dsr2.2007.07.028>, 2007.

795 Barron, J. A., Stickley, C. E., and Bukry, D.: Paleoceanographic, and paleoclimatic constraints on the global Eocene diatom and silicoflagellate record, Palaeogeography, Palaeoclimatology, Palaeoecology, 422, 85–100, <https://doi.org/10.1016/j.palaeo.2015.01.015>, 2015.

800 | **Bohaty, S. M. and Zachos, J. C.: Significant Southern Ocean warming event in the late middle Eocene, Geology, 31, 1017–1020, https://doi.org/10.1130/G19800.1, 2003.**

Borreli, C., Cramer, B. S., and Katz, M. E.: Bipolar Atlantic deepwater circulation in the middle-late Eocene: Effects of Southern Ocean gateway openings, Paleoceanography, 29, 308–327, <https://doi.org/10.1002/2012PA002444>, 2014.

805 Bryłka, K., Witkowski, J., and Bohaty, S. M.: Biogenic silica accumulation and diatom assemblage variations through the Eocene-Oligocene Transition: A Southern Indian Ocean versus South Atlantic perspective, Palaeogeography, Palaeoclimatology, Palaeoecology, 636, 111971, <https://doi.org/10.1016/j.palaeo.2023.111971>, 2024.

810 Cabrera-Brufau, M., Arin, L., Sala, M. M., Cermeño, P., and Marrasé, C.: Diatom dominance enhances resistance of phytoplanktonic POM to mesopelagic microbial decomposition, Frontiers in Marine Science, 8, <https://doi.org/10.3389/fmars.2021.683354>, 2021.

810 Chapman, C. C., Lea, M. A., Meyer, A., Sallée, J.-B., and Hindell, M.: Defining Southern Ocean fronts and their influence on biological and physical processes in a changing climate, *Nat. Clim. Chang.*, 10, 209–219, <https://doi.org/10.1038/s41558-020-0705-4>, 2020.

Cortese, G., Gersonde, R., Hillenbrand, C.-D., and Kuhn, G.: Opal sedimentation shifts in the World Ocean over the last 15 Myr, *Earth and Planetary Science Letters*, 224, 509–527, <https://doi.org/10.1016/j.epsl.2004.05.035>, 2004.

815 Coxall, H. K. and Pearson, P. N.: The Eocene–Oligocene Transition, in: Deep-time perspectives on climate change: Marrying the signal from computer models and biological proxies, The Geological Society of London on behalf of The Micropalaeontological Society, 351–387, <https://doi.org/10.1144/tms002.16>, 2007.

820 Coxall, H. K., Wilson, P. A., Pälike, H., Lear, C. H., and Backman, J.: Rapid stepwise onset of Antarctic glaciation and deeper calcite compensation in the Pacific Ocean, *Nature*, 433, 53–57, <https://doi.org/10.1038/nature03135>, 2005.

DeConto, R. M. and Pollard, D.: Rapid Cenozoic glaciation of antarctica induced by declining atmospheric CO₂, *Nature*, 421, 245–249, <https://doi.org/10.1038/nature01290>, 2003.

825 Diekmann, B., Kuhn, G., Gersonde, R., and Mackensen, A.: Middle Eocene to early Miocene environmental changes in the sub-Antarctic Southern Ocean: Evidence from biogenic and terrigenous depositional patterns at ODP site 1090, *Global and Planetary Change*, 40, 295–313, <https://doi.org/10.1016/j.gloplacha.2003.09.001>, 2004.

830 [Diester-Haass, L. and Zahn, R.: Eocene-Oligocene transition in the Southern Ocean: History of water mass circulation and biological productivity, Geol.](https://doi.org/10.1130/0091-7613(1996)024%253C0163:etits%253E2.3.co;2) 24, 163, [https://doi.org/10.1130/0091-7613\(1996\)024%253C0163:etits%253E2.3.co;2](https://doi.org/10.1130/0091-7613(1996)024%253C0163:etits%253E2.3.co;2), 1996.

835 [Douglas, P. M. J., Affek, H. P., Ivany, L. C., Houben, A. J. P., Sijp, W. P., Sluijs, A., Schouten, S., and Pagani, M.: Pronounced zonal heterogeneity in Eocene southern high-latitude sea surface temperatures, Proc. Natl. Acad. Sci. U.S.A.](https://doi.org/10.1073/pnas.1321441111), 111, 6582–6587, <https://doi.org/10.1073/pnas.1321441111>, 2014.

Egan, K. E., Rickaby, R. E. M., Hendry, K. R., and Halliday, A. N.: Opening the gateways for diatoms primes earth for Antarctic glaciation, *Earth and Planetary Science Letters*, 375, 34–43, <https://doi.org/10.1016/j.epsl.2013.04.030>, 2013.

840 Ehrmann, W. U.: Implications of sediment composition on the southern Kerguelen Plateau for paleoclimate and depositional environment, in: Proceedings of the ocean drilling program, 119 scientific results, Ocean Drilling Program, <https://doi.org/10.2973/odp.proc.sr.119.121.1991>, 1991.

845 Ehrmann, W. U. and Mackensen, A.: Sedimentological evidence for the formation of an east Antarctic ice sheet in Eocene/Oligocene time, *Palaeogeography, Palaeoclimatology, Palaeoecology*, 93, 85–112, [https://doi.org/10.1016/0031-0182\(92\)90185-8](https://doi.org/10.1016/0031-0182(92)90185-8), 1992.

850 Elsworth, G., Galbraith, E., Halverson, G., and Yang, S.: Enhanced weathering and CO₂ drawdown caused by latest Eocene strengthening of the Atlantic meridional overturning circulation, *Nature Geoscience*, 10, 213–216, <https://doi.org/10.1038/ngeo2888>, 2017.

855 Evangelinos, D., Escutia, C., Flierdt, T. van de, Valero, L., Flores, J.-A., Harwood, D. M., Hoem, F. S., Bijl, P., Etourneau, J., Kreissig, K., Nilsson-Kerr, K., Holder, L., López-Quirós, A., and Salabarnada, A.: Absence of a strong, deep-reaching antarctic circumpolar current zonal flow across the Tasmanian gateway during the Oligocene to early Miocene, *Global and Planetary Change*, 208, 103718, <https://doi.org/10.1016/j.gloplacha.2021.103718>, 2022.

860 Evangelinos, D., Etourneau, J., Van De Flierdt, T., Crosta, X., Jeandel, C., Flores, J.-A., Harwood, D. M., Valero, L., Ducassou, E., Sauermilch, I., Klocker, A., Cacho, I., Pena, L. D., Kreissig, K., Benoit, M., Belhadj, M., Paredes, E., Garcia-Solsona, E., López-Quirós, A., Salabarnada, A., and Escutia, C.: Late Miocene onset of the modern Antarctic Circumpolar Current, *Nat. Geosci.*, <https://doi.org/10.1038/s41561-023-01356-3>, 2024.

865 Farmer, J. R., Hertzberg, J. E., Cardinal, D., Fietz, S., Hendry, K., Jaccard, S. L., Paytan, A., Rafter, P. A., Ren, H., Somes, C. J., Sutton, J. N., and GEOTRACES-PAGES Biological Productivity Working Group Members: Assessment of C, N and Si isotopes as tracers of past ocean nutrient and carbon cycling, *Global Biogeochem Cycles*, <https://doi.org/10.1029/2020GB006775>, 2021.

870 **Faul, K. L. and Delaney, M. L.: A comparison of early Paleogene export productivity and organic carbon burial flux for Maud Rise, Weddell Sea, and Kerguelen Plateau, south Indian Ocean, *Paleoceanography*, 25, <https://doi.org/10.1029/2009PA001916>, 2010.**

Funakawa, S. and Nishi, H.: Radiolarian faunal changes during the Eocene-Oligocene transition in the Southern Ocean (maud rise, ODP leg 113, site 689) and its significance in paleoceanographic change, *Micropaleontology*, 54, 15–26, <https://doi.org/10.47894/mpal.54.1.03>, 2008.

875 [Gasson, E., Lunt, D. J., DeConto, R., Goldner, A., Heinemann, M., Huber, M., LeGrande, A. N., Pollard, D., Sagoo, N., Siddall, M., Winguth, A., and Valdes, P. J.: Uncertainties in the modelled CO₂ threshold for Antarctic glaciation, Clim. Past, 10, 451–466, https://doi.org/10.5194/cp-10-451-2014, 2014.](#)

Hatton, I. A., Mazzarisi, O., Altieri, A., and Smerlak, M.: Diversity begets stability: Sublinear growth and competitive coexistence across ecosystems, *Science*, 383, <https://doi.org/10.1126/science.adg8488>, 2024.

880 Hodel, F., Grespan, R., De Rafélis, M., Dera, G., Lezin, C., Nardin, E., Rouby, D., Aretz, M., Steinmann, M., Buatier, M., Lacan, F., Jeandel, C., and Chavagnac, V.: Drake Passage gateway opening and Antarctic Circumpolar Current onset 31 Ma ago: The message of foraminifera and reconsideration of the Neodymium isotope record, *Chemical Geology*, 570, 120171, <https://doi.org/10.1016/j.chemgeo.2021.120171>, 2021.

885 [Hodel, F., Fériot, C., Dera, G., De Rafélis, M., Lezin, C., Nardin, E., Rouby, D., Aretz, M., Antonio, P., Buatier, M., Steinmann, M., Lacan, F., Jeandel, C., and Chavagnac, V.: Eocene-Oligocene southwest Pacific Ocean paleoceanography new insights from foraminifera chemistry \(DSDP site 277, Campbell Plateau\), Front. Earth Sci., 10, 998237, https://doi.org/10.3389/feart.2022.998237, 2022.](#)

890 [Houben, A. J. P., Bijl, P. K., Sluijs, A., Schouten, S., and Brinkhuis, H.: Late Eocene Southern Ocean Cooling and Invigoration of Circulation Preconditioned Antarctica for Full-Scale Glaciation, Geochem Geophys Geosyst, 20, 2214–2234, https://doi.org/10.1029/2019GC008182, 2019.](#)

895 [Howard, W. R. and Prell, W. L.: Late quaternary surface circulation of the southern Indian Ocean and its relationship to orbital variations, Paleoceanography, 7, 79–117, https://doi.org/10.1029/91pa02994, 1992.](#)

900 Hutchinson, D. K., Coxall, H. K., Lunt, D. J., Steinhorsdottir, M., Boer, A. M. de, Baatsen, M., Heydt, A. von der, Huber, M., Kennedy-Asser, A. T., Kunzmann, L., Ladant, J.-B., Lear, C. H., Moraweck, K., Pearson, P. N., Piga, E., Pound, M. J., Salzmann, U., Scher, H. D., Sijp, W. P., Śliwińska, K. K., Wilson, P. A., and Zhang, Z.: The Eocene–oligocene transition: A review of marine and terrestrial proxy data, models and model–data comparisons, *Climate of the Past*, 17, 269–315, <https://doi.org/10.5194/cp-17-269-2021>, 2021.

905 Kennett, J. P.: Cenozoic evolution of Antarctic glaciation, the circum-Antarctic Ocean, and their impact on global paleoceanography, *J. Geophys. Res.*, 82, 3843–3860, <https://doi.org/10.1029/JC082i027p03843>, 1977.

910 [Klages, J. P., Hillenbrand, C.-D., Bohaty, S. M., Salzmann, U., Bickert, T., Lohmann, G., Knahl, H. S., Gierz, P., Niu, L., Titschack, J., Kuhn, G., Frederichs, T., Müller, J., Bauersachs, T., Larter, R. D., Hochmuth, K., Ehrmann, W., Nehrke, G., Rodríguez-Tovar, F. J., Schmiedl, G., Spezzaferri, S., Läufer, A., Lisker, F., Van De Flierdt, T., Eisenhauer, A., Uenzelmann-Neben, G., Esper, O., Smith, J. A., Pälike, H., Spiegel, C., Dziadek, R., Ronge, T. A., Freudenthal, T., and Gohl, K.: Ice sheet-free West Antarctica during peak early Oligocene glaciation, Science, 385, 322–327, <https://doi.org/10.1126/science.adj3931>, 2024.](https://doi.org/10.1126/science.adj3931)

915 Ladant, J.-B., Donnadieu, Y., and Dumas, C.: Links between CO₂, glaciation and water flow: Reconciling the Cenozoic history of the Antarctic circumpolar current, *Climate of the Past*, 10, 1957–1966, <https://doi.org/10.5194/cp-10-1957-2014>, 2014.

920 Lauretano, V., Kennedy-Asser, A. T., Korasidis, V. A., Wallace, M. W., Valdes, P. J., Lunt, D. J., Pancost, R. D., and Naafs, B. D. A.: Eocene to Oligocene terrestrial southern hemisphere cooling caused by declining pCO₂, *Nature Geoscience*, 14, 659–664, <https://doi.org/10.1038/s41561-021-00788-z>, 2021.

925 Lazarus, D.: An improved cover-slip holder for preparing microslides of randomly distributed particles, *Journal of Sedimentary Research*, 64, 686–0, <https://doi.org/10.2110/jsr.64.686>, 1994.

930 Lazarus, D., Hollis, C. J., and Apel, M.: Patterns of opal and radiolarian change in the Antarctic mid-Paleogene: Clues to the origin of the Southern Ocean, *Micropaleontology*, 54, 41–48, <https://doi.org/10.47894/mpal.54.1.05>, 2008.

935 Lazarus, D., Barron, J., Renaudie, J., Diver, P., and Türke, A.: Cenozoic planktonic marine diatom diversity and correlation to climate change, *PLoS ONE*, 9, e84857, <https://doi.org/10.1371/journal.pone.0084857>, 2014.

940 Lear, C. H., Bailey, T. R., Pearson, P. N., Coxall, H. K., and Rosenthal, Y.: Cooling and ice growth across the Eocene-Oligocene transition, *Geology*, 36, 251–254, <https://doi.org/10.1130/G24584A.1>, 2008.

945 Liu, Z., Pagani, M., Zinniker, D., DeConto, R., Huber, M., Brinkhuis, H., Shah, S. R., Leckie, R. M., and Pearson, A.: Global Cooling During the Eocene-Oligocene Climate Transition, *Science*, 323, 1187–1190, <https://doi.org/10.1126/science.1166368>, 2009.

950 Livermore, R., Hillenbrand, C., Meredith, M., and Eagles, G.: Drake passage and Cenozoic climate: An open and shut case?, *Geochemistry, Geophysics, Geosystems*, 8, <https://doi.org/10.1029/2005gc001224>, 2007.

Mackensen, A.: Changing Southern Ocean palaeocirculation and effects on global climate, *Antarctic Science*, 16, 369–386, <https://doi.org/10.1017/s0954102004002202>, 2004.

Malviya, S., Scalco, E., Audic, S., Vincent, F., Veluchamy, A., Poulain, J., Wincker, P., Iudicone, D., De Vargas, C., Bittner, L., Zingone, A., and Bowler, C.: Insights into global diatom distribution and diversity in the world's ocean, *Proc. Natl. Acad. Sci. U.S.A.*, 113, <https://doi.org/10.1073/pnas.1509523113>, 2016.

Mittelbach, G. G., Scheiner, S. M., and Steiner, C. F.: What Is the Observed Relationship Between Species Richness and Productivity? Reply, Ecology, 84, 3390–3395, https://doi.org/10.1890/03-3077, 2003.

Müller, R. D., Cannon, J., Qin, X., Watson, R. J., Gurnis, M., Williams, S., Pfaffelmoser, T., Seton, M., Russell, S. H. J., and Zahirovic, S.: GPlates: Building a Virtual Earth Through Deep Time, Geochem. Geophys. Geosy., 19, 2243–2261, https://doi.org/10.1029/2018GC007584, 2018

955 Nilsen, E. B., Anderson, L. D., and Delaney, M. L.: Paleoproductivity, nutrient burial, climate change and the carbon cycle in the western equatorial Atlantic across the Eocene/Oligocene boundary: EOCENE/OLIGOCENE PRODUCTIVITY, *Paleoceanography*, 18, n/a-n/a, <https://doi.org/10.1029/2002PA000804>, 2003.

960 Özen, V., Renaudie, J., and Lazarus, D.: Unraveling Southern Ocean Diatom Diversity Across the Eocene/Oligocene Transition, *the Journal of Micropalaeontology*, subm.

Özen, V., Lazarus, D., Renaudie, J., & Faria, G.: Increasing opal productivity in the Late Eocene Southern Ocean: Evidence for increased carbon export preceding the Eocene-Oligocene glaciation [Data set]. Zenodo. <https://doi.org/10.5281/zenodo.14826336>, 2025

965 Pascher, K. M., Hollis, C. J., Bohaty, S. M., Cortese, G., McKay, R. M., Seebeck, H., Suzuki, N., and Chiba, K.: Expansion and diversification of high-latitude radiolarian assemblages in the late Eocene linked to a cooling event in the southwest Pacific, *Clim. Past*, 11, 1599–1620, <https://doi.org/10.5194/cp-11-1599-2015>, 2015.

970 **Paxman, G. J. G., Jamieson, S. S. R., Hochmuth, K., Gohl, K., Bentley, M. J., Leitchenkov, G., and Ferraccioli, F.: Reconstructions of Antarctic topography since the Eocene–Oligocene boundary, Palaeogeography, Palaeoclimatology, Palaeoecology, 535, 109346, https://doi.org/10.1016/j.palaeo.2019.109346, 2019.**

975 Plancq, J., Mattioli, E., Pittet, B., Simon, L., and Grossi, V.: Productivity and sea-surface temperature changes recorded during the late Eocene early Oligocene at DSDP Site 511 (South Atlantic), *Palaeogeography, Palaeoclimatology, Palaeoecology*, 407, 34–44, <https://doi.org/10.1016/j.palaeo.2014.04.016>, 2014.

R. Rintoul, S., W. Hughes, C., and Olbers, D.: Chapter 4.6 The antarctic circumpolar current system, in: International Geophysics, vol. 77, Elsevier, 271–XXXVI, https://doi.org/10.1016/S0074-6142(01)80124-8, 2001.

980 Rabosky, D. L. and Sorhannus, U.: Diversity dynamics of marine planktonic diatoms across the Cenozoic, *Nature*, 457, 183–186, https://doi.org/10.1038/nature07435, 2009.

985 Ragueneau, O., Tréguer, P., Leynaert, A., Anderson, R. F., Brzezinski, M. A., DeMaster, D. J., Dugdale, R. C., Dymond, J., Fischer, G., François, R., Heinze, C., Maier-Reimer, E., Martin-Jézéquel, V., Nelson, D. M., and Quéguiner, B.: A review of the Si cycle in the modern ocean: Recent progress and missing gaps in the application of biogenic opal as a paleoproductivity proxy, *Global and Planetary Change*, 26, 317–365, [https://doi.org/10.1016/S0921-8181\(00\)00052-7](https://doi.org/10.1016/S0921-8181(00)00052-7), 2000.

990 Ragueneau, O., Schultes, S., Bidle, K., Claquin, P., and Moriceau, B.: Si and C interactions in the world ocean: Importance of ecological processes and implications for the role of diatoms in the biological pump: Si AND C INTERACTIONS IN THE OCEAN, *Global Biogeochem. Cycles*, 20, <https://doi.org/10.1029/2006GB002688>, 2006.

Renaudie, J.: Quantifying the Cenozoic marine diatom deposition history: Links to the C and Si cycles, *Biogeosciences*, 13, 6003–6014, <https://doi.org/10.5194/bg-13-6003-2016>, 2016.

995 Renaudie, J., Lazarus, D., and Diver, P.: NSB (Neptune Sandbox Berlin): An expanded and improved database of marine planktonic microfossil data and deep-sea stratigraphy, *Palaeontologia Electronica*, <https://doi.org/10.26879/1032>, 2020.

1000 Renaudie, J., Lazarus, D., and Diver, P.: Archive of Neptune (NSB) database backups, <https://doi.org/10.5281/ZENODO.10063218>, 2023.

Robert, C., Diester-Haass, L., and Chamley, H.: Late Eocene–Oligocene oceanographic development at southern high latitudes, from terrigenous and biogenic particles: A comparison of Kerguelen Plateau and Maud Rise, ODP Sites 744 and 689, *Marine Geology*, 191, 37–54, [https://doi.org/10.1016/S0025-3227\(02\)00508-X](https://doi.org/10.1016/S0025-3227(02)00508-X), 2002.

1005

Rodrigues de Faria, G., Lazarus, D., Renaudie, J., Stammeier, J., Özen, V., and Struck, U.: Late eocene to early oligocene productivity events in the proto-Southern Ocean and correlation to climate change, *Climate of the Past*, 20, 1327–1348, <https://doi.org/10.5194/cp-20-1327-2024>, 2024.

1010 Salamy, K. A. and Zachos, J. C.: Latest Eocene-Early Oligocene climate change and Southern Ocean fertility: Inferences from sediment accumulation and stable isotope data, *Palaeogeography, Palaeoclimatology, Palaeoecology*, 145, 61–77, [https://doi.org/10.1016/S0031-0182\(98\)00093-5](https://doi.org/10.1016/S0031-0182(98)00093-5), 1999.

1015 **Sarkar, S., Basak, C., Frank, M., Berndt, C., Huuse, M., Badhani, S., and Bialas, J.: Late Eocene onset of the Proto-Antarctic Circumpolar Current, *Sci Rep*, 9, 10125, <https://doi.org/10.1038/s41598-019-46253-1>, 2019.**

1020 **Sauermilch, I., Whittaker, J. M., Klocker, A., Munday, D. R., Hochmuth, K., Bijl, P. K., and LaCasce, J. H.: Gateway-driven weakening of ocean gyres leads to Southern Ocean cooling, *Nat Commun*, 12, <https://doi.org/10.1038/s41467-021-26658-1>, 2021.**

1025 Scher, H. D. and Martin, E. E.: Timing and Climatic Consequences of the Opening of Drake Passage, *Science*, 312, 428–430, <https://doi.org/10.1126/science.1120044>, 2006.

1030 Scher, H. D., Bohaty, S. M., Zachos, J. C., and Delaney, M. L.: Two-stepping into the icehouse: East Antarctic weathering during progressive ice-sheet expansion at the Eocene-Oligocene transition, *Geology*, 39, 383–386, <https://doi.org/10.1130/G31726.1>, 2011.

1035 Scher, H. D., Bohaty, S. M., Smith, B. W., and Munn, G. H.: Isotopic interrogation of a suspected late Eocene glaciation: Hidden glaciation revealed in the Eocene, *Paleoceanography*, 29, 628–644, <https://doi.org/10.1002/2014pa002648>, 2014.

1040 Schumacher, S. and Lazarus, D.: Regional differences in pelagic productivity in the late Eocene to early Oligocene comparison of southern high latitudes and lower latitudes, *Palaeogeography, Palaeoclimatology, Palaeoecology*, 214, 243–263, [https://doi.org/10.1016/S0031-0182\(04\)00424-9](https://doi.org/10.1016/S0031-0182(04)00424-9), 2004.

1045 Shackleton, N. J. and Kennett, J. P.: Paleotemperature history of the Cenozoic and the initiation of Antarctic glaciation: Oxygen and carbon isotope analyses in DSDP sites 277, 279 and 281, in: *Initial reports of the deep-sea drilling project*, 29, U.S. Government Printing Office, <https://doi.org/10.2973/dsdp.proc.29.117.1975>, 1975.

1040 | Shipboard Scientific Party: Site 511. In: Initial Reports of the Deep-Sea Drilling Project, edited by Ludwig, W. J., Krasheninnikov, V. A. et al., 71: Washington (U.S. Govt. Printing Office). 1983.

1045 | Shipboard Scientific Party: Site 689. In: Proceedings of the Ocean Drilling Program, Initial Reports, edited by Barker, P. R, Kennett, J. P., et al, 113: College Station, TX (Ocean Drilling Program). 1988.

1050 | Shipboard Scientific Party: Site 748. In: Proceedings of the Ocean Drilling Program, Initial Reports, edited by Schlich, R., Wise, S. W., Jr., et al., 120: College Station, TX (Ocean Drilling Program) 1989.

1055 | Shipboard Scientific Party: Site 1090. In: Proceedings of the Ocean Drilling Program, Initial Reports edited by Gersonde, R., Hodell, D.A., Blum, P., et al., 177: College Station, TX (Ocean Drilling Program) 1998.

1060 | Stickley, C. E., Brinkhuis, H., Schellenberg, S. A., Sluijs, A., Röhl, U., Fuller, M., Grauert, M., Huber, M., Warnaar, J., and Williams, G. L.: Timing and nature of the deepening of the Tasmanian Gateway, Paleoceanography, 19, 2004PA001022, <https://doi.org/10.1029/2004PA001022>, 2004.

1065 | Sigman, D.M. and Hain, M.P. (2012) The biological productivity of the ocean. Nature Education Knowledge, 3 (6), 1-16.
Sijp, W. P., England, M. H., and Huber, M.: Effect of the deepening of the Tasman gateway on the global ocean, Paleoceanography, 26, <https://doi.org/10.1029/2011pa002143>, 2011.

1070 | Smetacek, V.: Diatoms and the ocean carbon cycle, Protist, 150, 25-32, [https://doi.org/10.1016/s1434-4610\(99\)70006-4](https://doi.org/10.1016/s1434-4610(99)70006-4), 1999.

Stickley, C. E., Brinkhuis, H., Schellenberg, S. A., Sluijs, A., Röhl, U., Fuller, M., Grauert, M., Huber, M., Warnaar, J., and Williams, G. L.: Timing and nature of the deepening of the Tasmanian Gateway: Deepening of the Tasmanian Gateway, Paleoceanography, 19, n/a-n/a, <https://doi.org/10.1029/2004PA001022>, 2004.

Straume, E. O., Nummelin, A., Gaina, C., and Nisancioglu, K. H.: Climate transition at the Eocene Oligocene influenced by bathymetric changes to the Atlantic Arctic oceanic gateways, Proceedings of the National Academy of Sciences, 119, e2115346119, <https://doi.org/10.1073/pnas.2115346119>, 2022.

Ted C. Moore: Method of randomly distributing grains for microscopic examination, J. Sediment. Res., 43, <https://doi.org/10.1306/74d728ba-2b21-11d7-8648000102c1865d>, 1973.

1075 Toumoulin, A., Donnadieu, Y., Ladant, J.-B., Batenburg, S. J., Poblete, F., and Dupont-Nivet, G.: Quantifying the Effect of the Drake Passage Opening on the Eocene Ocean, *Paleoceanography and Paleoclimatology*, 35, e2020PA003889, <https://doi.org/10.1029/2020PA003889>, 2020.

1080 Tréguer, P., Nelson, D. M., Van Bennekom, A. J., DeMaster, D. J., Leynaert, A., and Quéguiner, B.: The silica balance in the world ocean: A reestimate, *Science*, 268, 375–379, <https://doi.org/10.1126/science.268.5209.375>, 1995.

1085 Tréguer, P., Bowler, C., Moriceau, B., Dutkiewicz, S., Gehlen, M., Aumont, O., Bittner, L., Dugdale, R., Finkel, Z., Iudicone, D., Jahn, O., Guidi, L., Lasbleiz, M., Leblanc, K., Levy, M., and Pondaven, P.: Influence of diatom diversity on the ocean biological carbon pump, *Nature Geoscience*, 11, 27–37, <https://doi.org/10.1038/s41561-017-0028-x>, 2018.

1090 Villa, G., Fioroni, C., Pea, L., Bohaty, S., and Persico, D.: Middle Eocene–late Oligocene climate variability: Calcareous nannofossil response at Kerguelen Plateau, Site 748, *Marine Micropaleontology*, 69, 173–192, <https://doi.org/10.1016/j.marmicro.2008.07.006>, 2008.

1095 Villa, G., Fioroni, C., Persico, D., Roberts, A. P., and Florindo, F.: Middle Eocene to Late Oligocene Antarctic glaciation/deglaciation and Southern Ocean productivity, *Paleoceanography*, 29, 223–237, <https://doi.org/10.1002/2013PA002518>, 2014.

1100 Virta, L., Gammal, J., Järnström, M., Bernard, G., Soininen, J., Norkko, J., and Norkko, A.: The diversity of benthic diatoms affects ecosystem productivity in heterogeneous coastal environments, *Ecology*, 100, e02765, <https://doi.org/10.1002/ecy.2765>, 2019.

Wade, B. S., O'Neill, J. F., Phujareanchaiwon, C., Ali, I., Lyle, M., and Witkowski, J.: Evolution of deep-sea sediments across the Paleocene-Eocene and Eocene-Oligocene boundaries, *Earth-Science Reviews*, 211, 103403, <https://doi.org/10.1016/j.earscirev.2020.103403>, 2020.

1105 Westacott, S., Planavsky, N. J., Zhao, M.-Y., and Hull, P. M.: Revisiting the sedimentary record of the rise of diatoms, *Proceedings of the National Academy of Sciences*, 118, <https://doi.org/10.1073/pnas.2103517118>, 2021.

Westerhold, T., Marwan, N., Drury, A. J., Liebrand, D., Agnini, C., Anagnostou, E., Barnet, J. S. K., Bohaty, S. M., De Vleeschouwer, D., Florindo, F., Frederichs, T., Hodell, D. A., Holbourn, A. E., Kroon, D., Lauretano, V., Littler, K., Lourens, L. J., Lyle, M., Pälike, H., Röhl, U., Tian, J., Wilkens, R. H., Wilson, P. A., and Zachos, J. C.: An astronomically

dated record of Earth's climate and its predictability over the last 66 million years, *Science*, 369, 1383–1387, <https://doi.org/10.1126/science.aba6853>, 2020.

1110 [**Wilson, D. S. and Luyendyk, B. P.: West Antarctic paleotopography estimated at the Eocene–Oligocene climate transition, *Geophysical Research Letters*, 36, https://doi.org/10.1029/2009gl039297, 2009.**](#)

1115 [**Wilson, D. S., Pollard, D., DeConto, R. M., Jamieson, S. S. R., and Luyendyk, B. P.: Initiation of the West Antarctic Ice Sheet and estimates of total Antarctic ice volume in the earliest Oligocene, *Geophysical Research Letters*, 40, 4305–4309, https://doi.org/10.1002/grl.50797, 2013.**](#)

Witkowski, J., Bohaty, S. M., McCartney, K., and Harwood, D. M.: Enhanced siliceous plankton productivity in response to middle Eocene warming at Southern Ocean ODP Sites 748 and 749, *Palaeogeography, Palaeoclimatology, Palaeoecology*, 326–328, 78–94, <https://doi.org/10.1016/j.palaeo.2012.02.006>, 2012.

1120 Witkowski, J., Brylka, K., Bohaty, S. M., Mydłowska, E., Penman, D. E., and Wade, B. S.: North Atlantic marine biogenic silica accumulation through the early to middle Paleogene: Implications for ocean circulation and silicate weathering feedback, *Climate of the Past*, 17, 1937–1954, <https://doi.org/10.5194/cp-17-1937-2021>, 2021.

1125 Zachos, J. and Kump, L.: Carbon cycle feedbacks and the initiation of Antarctic glaciation in the earliest Oligocene, *Global and Planetary Change*, 47, 51–66, <https://doi.org/10.1016/j.gloplacha.2005.01.001>, 2005.

Zachos, J., Pagani, M., Sloan, L., Thomas, E., and Billups, K.: Trends, rhythms, and aberrations in global climate 65 Ma to present, *Science*, 292, 686–693, <https://doi.org/10.1126/science.1059412>, 2001.

1130 Zachos, J. C., Quinn, T. M., and Salamy, K. A.: High-resolution (104 years) deep-sea foraminiferal stable isotope records of the Eocene-Oligocene climate transition, *Paleoceanography*, 11, 251–266, <https://doi.org/10.1029/96pa00571>, 1996.

1135 Zhang, Y. G., Pagani, M., Liu, Z., Bohaty, S. M., and DeConto, R.: A 40-million-year history of atmospheric CO₂, *Philosophical Transactions of the Royal Society A: Mathematical, Physical and Engineering Sciences*, 371, 20130096, <https://doi.org/10.1098/rsta.2013.0096>, 2013.